

Coupling between chromophoric dissolved organic matter and dissolved inorganic carbon in Indian estuaries

Nittala S Sarma^{1,*}, G Cthiranjeevulu¹, Sudarsana Rao Pandi^{1,a}, Dokala Bhaskara Rao^{1,b}, VVSS Sarma²

1. Marine Chemistry Laboratory, Department of Chemistry, Andhra University, Visakhapatnam-530003, India

2. CSIR-National Institute of Oceanography Regional Centre, 176 Lawsons Bay Colony, Visakhapatnam-530017, India.

a. Present address: National Centre for Polar and Ocean Research, Ministry of Earth Sciences, Vasco-da-Gama, Goa - 403804, India

b. Present address: Centre for Marine Living Resources and Ecology (CMLRE), Atal Bhavan, Ministry of Earth Sciences, LNG Road, Puthuvypin South, Kochi-682508

*Address for correspondence, Email: sarmanittala@gmail.com

Abstract

This study investigates the coupling between Chromophoric Dissolved Organic Matter (CDOM) and Dissolved Inorganic Carbon (DIC) in eighteen Indian estuaries across salinity gradient of the east and west coasts during the monsoon season, characterized by significant river discharge. The hypothesis that humic acids (HA) and fulvic acids (FA), prominent in estuarine CDOM, closely correspond to the 'organic alkalinity' (A_{org}) component of total alkalinity is explored. In most estuaries, specifically those along the northeast coast (NE) and southwest coast (SW), a significant linear relationship exists between DIC, CDOM abundance, and pH level. Notably, minor estuaries along the southeast coast (SE) and northwest coast (NW) exhibit elevated DIC levels beyond what this relationship predicts. These estuaries also reveal heightened ammonium levels, increased $\delta^{15}N$ values, and decreased $\delta^{13}C$ values, indicative of anthropogenic influence. CDOM properties, such as spectral slope ($S_{300-500}$) and spectral slope ratio (SR , $S_{275-295}:S_{350-400}$), align with these findings, with SE and NW estuaries displaying higher values. On average, CDOM contributes 110.5 μM (6.8%) to DIC in NE, 390.7 μM (11%) in SE, 24.4 μM (4.8%) in SW, and 122.2 μM (4%) in NW estuaries. The relationship between total alkalinity minus DIC (TA-DIC) and pH_{25} suggests that CDOM, mediated by HA/FA, buffers the inorganic carbon system in estuaries. This buffering capacity weakens with elevated DIC levels, and this condition is marked by anomalous SR values compared to the baseline salinity- SR linear regression. This Study suggests that estuarine CDOM could largely represent "organic alkalinity" and could help monitor acidification in estuaries.

Keywords: Chromophoric/colored dissolved organic matter, CDOM; Indian Ocean; Dissolved Inorganic Carbon, DIC, $CO_2(aq)+HCO_3^-+CO_3^{2-}$; H_4SiO_4 ; Ocean acidification, OA; Organic alkalinity, A_{org}

Introduction

In the classical treatment of the seawater acid-base system, inorganic species play a pivotal role in determining total alkalinity (TA) and charge balance alkalinity (Middelburg et al., 2020; Dickson et al., 1981). Oceanographically significant weak inorganic acids, such as bicarbonate (HCO_3^- , transitioning to CO_3^{2-} , $\text{pK}_a = 10.33$ at 25°C), silicic acid (H_4SiO_4 , H_3SiO_4^- , 9.8), ammonium (NH_4^+ , NH_3 , 9.24), boric acid (H_3BO_3 , H_4BO_4^- , 9.15), dihydrogen orthophosphate (H_2PO_4^- , HPO_4^{2-} , 7.21), hydrogen sulfide (H_2S , HS^- , 7.05), and carbonic acid (H_2CO_3 , HCO_3^- , 6.35), contribute to alkalinity (ACS, 2022). Weaker acids with higher pK_a values may also contribute if present in significant concentrations. Notably, the pK_a of Baltic dissolved organic matter (DOM) has been calculated as 7.27, and humic/fulvic substances within DOM have a pK_a around 6.5 (Hammer et al., 2017; Ulfsbo et al., 2015; Kuliński et al., 2014). These constituents contribute to alkalinity when the pH exceeds 4.3, below which H_2CO_3 remains undissociated. At approximately pH 3, CO_2 gas is liberated from H_2CO_3 solution due to the rapid decline of CO_2aq hydration, driven by the dehydration constant k_D of H_2CO_3 (~ 850 , Soli and Byrne, 2002). The pK_a of humic acids (HA) extracted from various sources ranges from 2.5 to 8.5 (Paul et al., 2015; Theng, 2012; Choppin and Kullberg, 1978; Visser, 1964), comparable to that of H_2CO_3 . Consequently, the high concentrations of organic acids in DOM could potentially contribute to seawater alkalinity, particularly in estuarine environments.

To account for the ionic balance under electrically neutral conditions, the concept of 'Organic alkalinity' (A_{org}) also called DOM alkalinity has gained increased attention in recent literature (Hunt et al., 2022; Cai et al., 2021; Kerr et al., 2021; Hu, 2020; Middelburg et al., 2020; Song et al., 2020). A_{org} 's quantitative significance is notable in riverine, estuarine, and coastal waters affected by river discharge due to the high presence of fulvic acids/humic acids (FA/HA), which constitute a dominant weak acid fraction in terrestrially sourced DOM. The concentrations of FA/HA decrease downstream in the estuary due to mixing with seawater from offshore, leading to a corresponding decrease in A_{org} (Hunt et al., 2022). Given their prevalence in terrigenous DOM, FA/HA are significantly increased in the reactive chromophoric dissolved organic matter (CDOM) of estuaries during high-flow events (Bhattacharya and Osburn, 2021). FA/HA are characterized by functional groups, such as $-\text{COOH}$ and $-\text{OH}$, within their aromatic molecular structures of varying molecular weights (MW, 10^2 to 3×10^5 , Mostofa et al., 2013; Perminova et al., 2003), enabling the formation of salts with cations stronger than the proton that they have to displace (e.g., Na^+ , K^+ , Ca^{2+} , Mg^{2+}) (Davies and Ghabbour, 1998). Depending on its heterotrophic activity tendency, anthropogenic DOM can strongly contribute to A_{org} , especially when metabolites are weakly acidic ($\text{pK}_a > 4.5$). The portion of the DOM pool resulting from in situ primary production and respiration is primarily dominated by sugars, proteins and

polymers reconstructed from their degradation or alteration products, making a relatively minor contribution to A_{org} (Ko et al., 2016).

Chromophoric dissolved organic matter (CDOM), a significant component of DOM absorbing UV-Visible light (Pandi et al., 2021a; Coble, 2007; Bricaud et al., 1981), serves as an accessible optical parameter for estimating dissolved organic carbon (DOC) concentration, particularly when autochthonous inputs are limited (Asmala et al., 2012; Fichot and Benner, 2011). As DOM composition varies across the river-coastal sea continuum due to biogeochemical, bacterial, and photochemical processes (Pandi et al., 2021a; Grunert et al., 2021; Fichot and Benner, 2012; Coble, 2007; Coble et al., 2004), CDOM can offer insights into these processes. Given the importance of monitoring changes in CO_2 absorption from or release to the atmosphere due to global warming, exploring whether CDOM can serve as a proxy for A_{org} and understanding the relationship between CDOM and DIC becomes interesting.

Additionally, organic inputs to estuaries contribute to acidification through heterotrophic activity on labile (bio-available) organic matter. The labile fraction of DOM primarily consists of protein-like substances, while the refractory fraction mainly comprises humic-like components (Hosen et al., 2014). Humic-like DOM acquired along rivers significantly controls DIC in both large and small rivers with minimal anthropogenic inputs. Variations in pH, alkalinity, buffering mechanisms, and structural distinctions within humic compounds (FA/HA) among different estuaries lead to diverse acidification and buffering scenarios. To assess ocean acidification rates, Xue and Cai (2020) proposed the difference between total alkalinity (TA) and DIC (TA–DIC) as a conservative tracer in ocean waters, albeit with a caution regarding its validity in low-saline (salinity $< 20 \times 10^{-3}$) estuarine waters and when (TA–DIC) is $< \sim 50 \mu\text{mol kg}^{-1}$ due to the non-linear trend in (TA–DIC) versus pH_{25} (pH at 25°C) (Xue and Cai, 2020).

In light of the aforementioned, this paper's primary objective is to test the hypothesis that humic acids (HA) and fulvic acids (FA), prevalent in estuarine CDOM, closely represent the 'organic acids'—the organic alkalinity fraction of total alkalinity (TA). To address this, we investigate the relationship between carbonate system species (e.g., dissolved inorganic carbon, DIC), aquatic weak acids (CDOM [HA]), H_4SiO_4 , pH, and TA. Additionally, we explore the behavior of these species under anthropogenic influence to propose CDOM as a measurable parameter for monitoring anthropogenic DOM input. Lastly, we aim to ascertain whether the (TA–DIC) metric holds relevance in estuarine acidification studies and whether CDOM plays a role in acidification.

2. Material and methods

2.1. Hydrogeographic details of the Indian estuaries

A total of 18 estuaries, 10 on the east coast (EC) of India (Bay of Bengal, BoB) and 8 on the west coast (WC, Arabian Sea, AS) were studied (Fig. 1). The hydro-geological characteristics including the size of the river, the composition of the drainage basin and factors e.g., anthropogenic that may potentially affect the water quality are given in Table S1. The tropical Indian rivers are monsoonal and experience heavy discharges during the main monsoon season (June-September). Discharges during the monsoon season control the overall discharge through rivers. The combined annual discharge of the 10 east flowing rivers is $\sim 342 \text{ km}^3$ and that of the 8 west flowing rivers is 106 km^3 (Table S1). The rainfall over the Indian subcontinent is not uniform due to the uneven nature of the coast flanked by the western and eastern ghats. The rainfall decreases in the sequence southwestern India (SW) > northeast (NE) > northwest (NW) > southeast (SE) during the summer (monsoon, June to September) season. The SE receives greater rainfall during the winter monsoon (November to February) (Soman and Kumar, 1990).

Subarnarekha (SR) is born on a plateau (near Ranchi) adjoining the eastern ghats. The larger rivers e.g., Mahanadi (MN), Godavari (GV), Krishna (KN), and Cauvery (CR) originate from the western ghats and traverse diverse terrains before joining the Bay of Bengal (Vaidyanathan, 2013). The river deltas are extensive on the EC. Shorter rivers originate in the eastern ghats e.g., Rushikulya (RK), Penna (PN), Ponnaiyar (PY) and Vellar (VL) and on the western slopes of the western ghats e.g., Mandovi (MV), Zuari (ZR), Kali (KL), Netravati (NV) and the rivers impounding into the Kochi backwater system (KC). Close to these estuaries, extensive agricultural activity as well as aquaculture, urbanization and industrial activity let in their wastes into the effluents that flow through them (Vaidyanathan, 2013). Seven rivers (out of 8) flowing into the Arabian Sea (AS) are minor. They are rift-valley rivers and do not give rise to deltas at their confluence with the Sea. Narmada (ND) is the longest. It takes birth in central India at the meeting point of Vindhya and Satpura hills. Tapi (TT) lying a little north of the western ghats and Mahisagar (MS) river which rises in the Vindhya mountains are small. Extensive industrial development based on petroleum resources has taken place off Mumbai-Okha coast (AS) which is dotted with these 3 rivers. The other rivers Mandovi, Zuari, Netravati and Kali (which originate in the Western ghats), drain mineral (metal)-rich terrains.

2.2. Sampling and onsite measurements:

Sampling of the 18 estuaries (Fig. 1) was done across the salinity gradient during 10th July -6th August 2014 when the southwest (SW) monsoon was active. The discharge was typically high in all

estuaries. Exception was of the southeastern (SE) estuaries (Penna, Ponnaiyar, Vellar and Cauvery) that have low discharge all year long because of limited contribution of SW monsoon over their catchment areas, although over the Indian Subcontinent, the share of SW monsoon to the overall rainfall is ~80%, and high water use upstream. Further, during 2014, the SW monsoon was particularly late because of which Krishna estuary (BoB) was experiencing low discharge at the time of sampling (Mangalaa et al., 2017).

Water samples were collected using mechanized vessels hired locally with 5 liter Niskin bottle. In each estuary, generally three to five samples were collected across the salinity gradient from near-zero salinity up to the mouth of the estuary. The mode of sampling was adapted to circumstances such as boat/ferry availability and accessibility (e.g. restrictions imposed by local authorities due to heavy discharge). Most samples were obtained from the middle of the stream but when not possible due to heavy flooding, directly from shore. The sampling was confined to surface (-1 m) uniformly. Temperature and salinity were measured by using portable CTD for some estuaries (Sea-Bird Electronics, SBE 19 plus, USA) and portable pH and conductivity electrodes (WTW, MultiLine P4) were used in other estuaries. The latter was calibrated with CTD to calculate the salinity.

2.3. Measurement of Alkalinity and DIC:

The pH was measured using glass electrodes (Metrohm, Zofingen, Switzerland) following standard operating procedures (DOE, 1998). TA was measured following Gran Titration method using autotitrator (Metrohm, Switzerland), DIC was measured using a coulometer (model CM 5014; UIC Inc., Joliet, IL, USA) interfaced to an automated subsampling system. The precisions for pH, TA and DIC were ± 0.002 , 2.5 mM and ± 1.8 mM, respectively. The accuracy of the pH, TA and DIC were estimated using Certified Reference Materials (0.015, 4.8 mM and 4 mM, respectively) supplied by Dr A.G. Dickson of Scripps Institute of Oceanography, USA.

2.4. CDOM sample handling and measurement:

The CDOM methodology was described earlier (Sarma et al., 2018; Chiranjeevulu et al., 2014; Pandi et al., 2014; Chari et al., 2013, 2012). Briefly, sub-samples were drawn from the sampler, first for CDOM in pre-cleaned (strong chromic acid, overnight) amber-colored bottles (100 ml) with Teflon screw caps following a thorough rinse. These samples, kept in ice boxes, were filtered at the earliest (mostly in less than an hour after collection) in the shore laboratory over Nucleopore filters (0.22 μ , Whatmann). The filtered samples were stored at 4°C in a refrigerator for <24 to 48 h after filtration, except when the samples were to be shipped (the northwestern, NW estuaries Narmada, Tapti and Mahisagar). Just before spectral measurement, the samples were filtered again applying a gentle

vacuum (to avoid microbubbles) as before, and the filtrates, after an equilibration time of 15 minutes (when the samples reached a constant temperature of $22\pm 1^\circ\text{C}$, and invisible microbubbles if any disappeared) were examined for their absorption spectra using the UV-Visible spectrophotometer (Shimadzu 1800, double beam, quartz cuvettes, path length, 100 mm) in the spectral range 200-800 nm at 1μ spectral resolution.

The absorbance spectra were null-point corrected at 700 nm for uniformity (Shank et al. 2005). The absorption coefficient $a(\lambda)$ was calculated from the corrected absorbance using the equation,

$$a(\lambda) = 2.303 A(\lambda) / 0.1 \text{ (m}^{-1}\text{)}$$

where 2.303 is $\text{Ln}(10)$ and 0.1 is the cuvette path length in meters. Spectral slope, S was calculated by fitting nonlinear (exponential) regression model of absorption coefficient on different wavelength ranges e.g., 300–500, 275-295 and 350-400 nm ($S_{300-500}$, $S_{275-295}$ and $S_{350-400}$ respectively). From the latter two, the spectral slope ratio (SR) was calculated as a proxy of DOM molecular weight (Pandi et al., 2021a; Helms et al., 2008). In this study, the CDOM absorption coefficient at 350 nm i.e., $a_{\text{CDOM}}(350)$ or called CDOM for simplicity, is used throughout.

2.5. Collection and analysis of Suspended Particulate Matter (SPM):

Depending on turbidity, 200 to 500 ml of water were filtered on a pre-weighed (dried at 300°C for 3 h preceded by rinsing in water) $0.2\mu\text{m}$ polycarbonate filter and weighed again after drying. The weight difference was taken as the suspended particulate matter (SPM). Another filtration was done of seawater (1 L) on GF/F ($\sim 0.7\mu$ Whatman) filters. The filters were dried at 60°C for at least 24 h. Filters were acid fumigated for 12 h in desiccator to remove inorganic carbon. The organic carbon on the filter (POC) was measured using elemental analyzer.

2.5.1. Stable Isotopes and Elemental Ratios

The content and the stable isotopic composition of carbon (^{12}C , ^{13}C) and nitrogen (^{14}N , ^{15}N) in the SPM were measured on elemental analyzer coupled with isotope ratio mass spectrometer (EA-IRMS-Delta V, Finnigan, Germany), and results are expressed relative to conventional standards, i.e., Vienna Pee Dee Belemnite (VPDB) for carbon (Coplen, 1996) and atmospheric N_2 for nitrogen (Mariotti, 1983), as δ values, defined as

$$\delta R = (X_{\text{sample}} - X_{\text{standard}}) / X_{\text{standard}} \times 10^3$$

where $R = ^{13}\text{C}$ or ^{15}N and $X = ^{13}\text{C}/^{12}\text{C}$ or $^{15}\text{N}/^{14}\text{N}$. The high-purity tanks CO_2 and N_2 were used as working standard for carbon and nitrogen. These gases were calibrated with internal reference materials of Glutamic Acid, Alanine, marine sediment, and International Atomic Energy Agency

(IAEA) standards. The long-term precision of the instrument is approximately $\pm 0.2\%$ for both C and N. It may be added that the subsamples for $\delta^{15}\text{N}$ analysis did not receive acid treatment as this has been reported to affect $\delta^{15}\text{N}$ values (Pinnegar and Polunin, 1999; Bunn et al., 1995; Goering et al., 1990).

2.6. Statistical analyses:

Statistical tests and all regressions were done in Microsoft Excel worksheets. The correlation criteria of the co-varying variables in the scatterplots, namely the number of cases (N), Pearson correlation coefficient (r) and its significance (p, two-tailed) are given within the relevant figures in sequence, along with the regression fit. The outliers had Y concentrations deviating from the predicted concentration by $>2\sigma$, where σ is the standard deviation of residuals of the regression best fit. The T-test was done using the IBM SPSS package available online ([T-Test Calculator for 2 Independent Means \(socscistatistics.com\)](http://www.socscistatistics.com)). Results with $p < 0.05$ were considered as significant.

2.7. Calculation of CDOM contributions to DIC:

The coefficients of CDOM (199.8369) and pH (934.6754) in the multiple linear regression model for DIC (Section 3.2.1) were multiplied with the respective concentrations (of CDOM and pH) of each sample, and the ratio of the products was considered as the ratio of contributions of the two (CDOM and pH) to DIC of that sample. From this ratio, the CDOM contribution to the observed DIC was calculated both as % value and in μM .

3. Results

Detailed distributions of different constituents and their mutual relationships, based on the consolidated data on all samples analyzed from the 18 estuaries are presented in the following. Where simplifying the account is needed to throw better clarity, the estuaries are divided as belonging to the 4 sectors NE, SE, SW and NW, as shown in Fig. 1.

3.1. Hydrochemistry

Salinity ranged from near nil to $>29 \times 10^{-3}$ at the stations sampled. The temperature and pH ranged from 24.6 to 34 °C and from 6.194 to 8.78, respectively. At corresponding salinities (i.e., close salinity bands of <2 , 2-5, 5-10, 10-15 and $15-20 \times 10^{-3}$), the NE estuarine water was, on average, warmer, of higher pH, more alkaline and richer in DIC than the SW estuarine water by 2.9° C, 0.48, 1030 μM and 948 μM (averages), respectively) (Table S2). In the SE and NW estuaries which are minor estuaries (except Narmada which is a major estuary), the concentrations of different constituents which are indicators of probable anthropogenic inputs e.g., NH_4^+ are elevated compared to the NE and SW estuaries. The NH_4^+ (Fig. S1a) had average concentrations of 5.11 μM (SE, N=14), 2.76 (NW, 12),

1.91 (SW, 18) and 0.83 μM (NE, 23) (Table S2). (The Cauvery estuary (SE) was not part of the SE average as it showed very low concentration of NH_4^+ (0.82 μM , $N=4$) than the other samples of SE estuaries, and a justification of this deviation is given in Section 4.2.)

The H_4SiO_4 was also higher in SE and NW than NE and SW estuaries (Fig. S1b, Table S2). POC and PON appeared to show a combined effect of monsoon and anthropogenic inputs (Fig. S1c,d). Due to anthropogenic influence, both POC and PON were highest in the SE ($91.16 \pm 105.97 \text{ mgL}^{-1}$ and 11.76 ± 16.45 respectively). The NE estuaries, and SW estuaries where the monsoon influence was high had less next. However, chl-a showed a mixed trend of enrichment under suitable (nutrient-enriched) conditions of anthropogenic inputs (SE) and natural inputs (SW) (Fig. S1e). $\delta^{13}\text{C}$ of POC (Fig. S1f) was marginally lower in the SE ($-25.37 \pm 1.85\text{‰}$) and NW ($-25.6 \pm 3.59\text{‰}$) estuaries compared to NE (-23.18 ± 1.36) and SW (-24.73 ± 1.43) estuaries. $\delta^{15}\text{N}$ (Fig. S1g) showed a mixed trend of highest depletion in SW ($8.07 \pm 2.43 \text{‰}$) and enrichment in NE estuaries ($11.90 \pm 3.89\text{‰}$). The SE and NW estuaries had intermediate depletion (9.30 ± 5.49 and $9.71 \pm 1.23\text{‰}$ in SE and NW estuaries respectively). DIC (Fig. 2a) was enriched in the SE and NW over NE and SW estuaries by 83% and 393% respectively, calculated from Table S2 data. TA also showed a wide disparity (Fig. S1h) like DIC. In NE and SW estuaries, pH related tightly to salinity ($R^2=0.95$, $N=24$, $p<0.0001$ and 0.90 , 20 , <0.0001) up to salinity 31.7 and 16.2×10^{-3} respectively (Fig. 2b) but not in the SE and NW estuaries (Fig. S2).

3.2. CDOM and its role in DIC:

The $a_{\text{CDOM}}(350)$, hereafter referred to as CDOM was examined to explore its role on DIC. CDOM was enriched in the SE estuaries compared to others (Fig. 2c). The highest CDOM 29.939 m^{-1} was observed at the upper estuary station of Ponnaiyar (SE). At 4 stations, it was in the range 6.93 to 10.755 m^{-1} . Considering 29.939 m^{-1} as an outlier ($>/<\text{average} \pm 2 \times \text{standard deviation, SD}$), the average CDOM of SE estuaries ($4.7827 \pm 2.9731 \text{ m}^{-1}$, 12 stations) was still the highest. The CDOM of SE was followed by that of NE and SW estuaries ($2.6772 \pm 0.8565 \text{ m}^{-1}$ and $1.6485 \pm 0.5917 \text{ m}^{-1}$ respectively). The NW estuaries in which NH_4^+ , TA and DIC were enriched (like in the case of SE estuaries), had the lowest CDOM ($1.4195 \pm 0.6480 \text{ m}^{-1}$, Table S2, Fig. 2c). The Spectral slope ($S_{300-500}$) was $0.0163 \pm 0.0011 \text{ nm}^{-1}$ and 0.0157 ± 0.0010 for the NE and SW estuaries respectively. The $S_{300-500}$ was somewhat higher in the SE than the NW estuaries (0.0172 ± 0.0005 and $0.0149 \pm 0.0014 \text{ nm}^{-1}$ respectively) (Table S2). The spectral slope ratio (SR , $S_{275-295}:S_{350-400}$ ratio) was examined as a more reliable indicator (than $S_{300-500}$) of changes at the molecular level (Fig. 2c). The SR was moderately lower in the SW estuaries than the NE estuaries. The highest SR was for the NW estuaries (1.23 ± 0.42) followed by the SE estuaries (1.10 ± 0.11) (Fig. 2c).

The CDOM related significantly to salinity in the NE estuaries ($R^2=0.50$, $N=25$, $p<0.0001$) (Fig. 3a) and in SW estuaries (0.35, 18, <0.01) but not in SE and NW estuaries (Fig. 3b). The seaward (downstream) samples (2) of the large Narmada estuary also aligned with the regression fit of SW estuaries (Fig. 3a). CDOM showed highly significant trends with H_4SiO_4 (Fig. 3c). H_4SiO_4 did not trend with DIC except in the SW estuaries (Fig. S3), but CDOM had a highly significant linear correlation to DIC ($R^2=0.73$, $N=45$, $p<0.0001$, Fig. 3d) i.e., in samples other than NW and the Krishna (NE) and Cauvery (SE) estuaries' samples which had higher DIC than predicted from the linear regression equation (Fig. 3d). (It may be recalled that NH_4^+ was particularly low in the cauvery estuary, Section 3.1). CDOM did not relate to DIC in SE and NW estuaries (Fig. 3d).

The *SR* correlated significantly with salinity in the NE+SW estuaries but not in SE+NW estuaries (Fig. 4a). With reference to the regression equation 1 for *SR* on salinity (Fig. 4a), the *SR* of both SE and NW estuaries was higher, by $29.1\% \pm 17.2\%$ ($N=18$).

$$SR = 0.0091\text{Salinity} + 0.8465 \quad (N=30, R^2 = 0.7048, p<0.0001) \dots \text{eq. 1}$$

SR also related to pH in both the NE+SW (Fig. S4) and SE+NW estuaries at high significance ($p<0.0001$; $R^2=0.45, 0.46$; $N=39, 23$ respectively) with 3 NW samples remaining as outliers (Fig. S4). *SR*, like CDOM, also held highly significant relationship to H_4SiO_4 and DIC (Fig. 4b,c). With reference to the regression line in Fig. 4c, the SE and NW outliers (2 and 5 respectively) of *SR* deviated between -25% and +92%.

3.2.1. Modelling of DIC from CDOM (and pH):

Although the relationship between CDOM and DIC was highly significant ($p<0.0001$, $N=45$, Fig. 3c), the root mean square error (RMSE) in the estimation of DIC was quite high (550 μM). Attempts were made to minimize RMSE and improve other statistical indices like significance and mean absolute per cent error (MAPE) by including other major acid-base parameters e.g., H_4SiO_4 and pH in multiple linear (regression) equations to predict DIC. Of all our attempts to develop a significant regression equation for DIC in the NE and SW estuaries which were influenced little by anthropogenic inputs, in terms of the commonly determined acid-base variables, a model involving pH and CDOM (eq. 2) produced minimum RMSE (260.2 μM of DIC), high significance (6.15×10^{-12}), low standard error (302.2 μM) and MAPE (21.5%) (Table S3).

$$\text{DIC } (\mu\text{m}) = -6288.05 + 934.6754\text{pH} + 199.8369\text{CDOM } (a_{350}, \text{m}^{-1}) \quad (p=6.15 \times 10^{-12}, N=37) \dots \text{eq. 2}$$

The predicted DIC matched with the observed DIC in NE and SW estuaries ($R^2=0.87$, $N=37$, $p<0.0001$) (Fig. 4d). In the SE and NW estuaries as well as the Krishna estuary (NE), which was

excluded from the model due to high DIC from the dam-released water, see above) the model estimated lower DIC. The contributions to DIC in eq. 2 of the two (independent) variables CDOM and pH, in μM and as % of DIC were calculated for each sample from the respective concentrations of CDOM and pH as presented in Section 2.6 (Fig. 5a,b). The contributions were higher in the CDOM-richer NE estuaries (averages, $110.5 \mu\text{M}$, 6.8%) compared to the SW estuaries ($24.4 \mu\text{M}$, 4.8%). The highest CDOM contributions were in the CDOM-richest SE samples ($390.7 \mu\text{M}$, 11%). The NW estuaries had concentrations ($122.2 \mu\text{M}$, 4%) that were similar to NE estuaries (although they contained less CDOM, see above). In all sectors, the CDOM contributions of DIC, generally decreased in the downstream direction. (Fig. 5a,b).

The eq. 2 also calculates that the pH would rise if CDOM were absent (assuming DIC as constant). The rise predicted is 0.63 from the current 7.68 in the NE estuaries (average DIC, $1484 \mu\text{M}$) and 0.31 from the current 7.05 in the SW estuaries (average DIC, $612 \mu\text{M}$). And that if the present pH remained unchanged, an increase of CDOM by 10% from its present average levels of 2.9338 m^{-1} (NE estuaries) and 1.6907 m^{-1} (SW) would cause the DIC to increase by $37.1 \mu\text{M}$ (2.5%, NE) and $67.1 \mu\text{M}$ (11.1%, NW). Similarly, a decrease of pH by 1% from its present average levels (7.68 and 7.05) would cause a decrease in the DIC by $93.3 \mu\text{M}$ and $32.6 \mu\text{M}$ i.e., by 6.2% and 5.4% in the NE and SW estuaries respectively, considering that the CDOM remained unchanged. Thus, the effect of perturbations in CDOM is felt significantly more in the SW estuaries than in NE estuaries.

3.2.2. DIC contributions directly from CDOM and pH:

The calculated DIC contribution from CDOM as per the model equation 2 was linearly correlated to CDOM highly significantly ($R^2=0.48$, $N=37$, $p<0.0001$ for the samples of the model (NE+SW, eq. 2). A tight relationship (0.91, 23, <0.00001) was shown by the samples not included in the model (SE+NW) (Fig. 5c). Similarly, the calculated DIC contribution from pH related (exponentially) to pH highly significantly in the modeled samples (NE and SE, 0.78, 22, <0.0001 ; 0.94, 17, <0.0001 respectively (Fig. 5d).

3.3. (TA-DIC) and its relation to pH_{25} and SR:

A plot of the distribution of the difference between TA and DIC (TA-DIC) versus pH_{25} was explored (Fig. 6a). The data were plotted as in the case of the Global Ocean Data Analysis Project Version 2 (GLODAPv2) database (Xue and Cai, 2020). The data trending similarly like the GLODAPv2 model (Xue and Cai, 2020) were first identified. More than half of the datapoints (34 of 66, 51.5%, mostly of NE and SE) appeared similar and gave rise to the linear regression equation (3) which was highly significant ($p<0.0001$). These samples were designated Class 1.

$$\text{pH}=0.001528(\text{TA-DIC}) + 7.4835 (R^2 = 0.6356) \dots (\text{eq. 3})$$

The group of data of nearly constant TA-DIC ($339.94 \pm 33.24 \mu\text{M}$) even as pH changed from 6.92 to 7.62 (Class 2) was identified in the remaining data (17 of 62, 25.8%). The further remaining data that remained after the preceding iterations (12 of 66, 18.2%) nicely fitted into another linear regression equation (4) which was highly significant ($p < 0.0001$). These samples were designated Class 3:

$$\text{pH} = 0.001584(\text{TA-DIC}) + 5.9588 (R^2 = 0.7740) \dots (\text{eq. 4}).$$

Three extreme negative data points of the NW estuaries, designated as Class 4, remained as outliers of the above three groups. The sample (analyte) source of each datapoint in all the four groups was noted. The Class 1 samples consisted of the EC estuaries and many SE samples. The Class 2 consisted mostly of the SW midstream samples (and some upstream exceptions of NE estuaries that did not conform to eq. 3. The Class 3 samples were mostly the WC upstream samples and Class 4, the NW exceptions. In Class 4 samples, DIC exceeded TA much; these samples were from the downstream Narmada estuary (TA-DIC=-313 ppm, Salinity=28.1) and midstream samples of Tapti estuary (2 samples, -805, 10.02 and -854, 20.11 respectively).

The 4 classes of samples were investigated to understand the nature of CDOM using *SR* as a proxy of CDOM structure. The *SR* increased versus (TA-DIC) with moderately high significance in both Class 1 ($p < 0.01$; $R^2=0.234$, $N=34$) and Class 3 (<0.01 , 0.53, 12) (Fig. 6b). In Class 2 of constant (TA-DIC) (339.94 ± 33.24), *SR* remained nearly constant (0.89 ± 0.06). In Class 4 samples in which DIC exceeded TA much, *SR* was very high for the Narmada downstream estuary sample (1.99) but very low for the Tapti midstream samples (0.84, 0.81). With reference to the salinity-*SR* regression line (eq. 1, Fig. 4a), the Narmada downstream sample's *SR* was higher by 79.2% and that of the Tapti lower by $18.2\% \pm 6.5\%$.

4. Discussion:

The division of Indian estuaries into the 4 sectors NE, SE, SW and NW has been in practice to account for organic pollution accompanied with high concentrations of N_2O , CH_4 and chl-a as well as lower rainfall in the SE and NW compared to NE and SW estuaries (Rao and Sarma, 2016, 2015; Khullar, 2014).

4.1. Chemical weathering could be influencing pH in NE and SW estuaries

The pH was higher in the NE estuaries than in the SW estuaries at corresponding salinities (Fig. 2b, Table S2). The pH of upstream water is a result of chemical weathering of the drainage basin, the rates of which are mainly affected by hydrology, lithology of the underlying bedrock, the overlying

soil, and water temperature (Hartmann et al., 2014, 2009). The pH of cloud water at equilibrium with atmospheric CO₂ is 5.6 (Charlson and Rodhe, 1982). The acidity of rainwater is neutralized by the cations (alkalinity) that enter the solution during weathering as shown in equation 5 for rock weathering (Schnoor and Stumm, 1986).



Feldspar

Kaolinite

The higher pH of the NE than the SW estuaries aligns with the higher magnitude of chemical weathering in them and a conservating of riverine and marine end-members. The NE rivers spend much longer time on land as they originate in the west coast of India and flow all the way to the east coast with average altitudes 1-2 orders of magnitude higher, and bring in much higher particulate load to the sea than the west-flowing rivers (Sarma et al., 2014; Vaidyanathan, 2013, Subramanian, 1993). Higher temperatures of NE over SW estuaries (Table S2) further enhance the weathering processes. In the west coast rivers, less modification takes place before the water reaches the estuaries, and the pH shifted lower due to the influence of rainwater (Nisha et al., 2021). The pH was higher at the downstream stations of the NE than SW estuaries, and is attributed to the higher pH of incoming seawater. A pH of ~8 is reported for the western BoB coastal water e.g., off Godavari estuary (Pandi et al., 2021b, Sarma et al., 2015) compared to the eastern AS coastal water, e.g., off Goa (Mandovi and Zuari estuaries) of ~7.5 (Shetye et al., 2020). The sediment deposits are also alkaline on the NE coast e.g., the clayey sand deposit of the ‘Haldia Terminal Site’ (IWAI, 2016).

The pH related weakly to salinity (up to a salinity of ~30 x 10⁻³) in the SE and NW estuaries, which may be due to the smaller size of the drainage basins of the rivers and similarity in the lithological and weathering factors. The Narmada (NW) which is long (1312 km), drains a variety of basins e.g., the Deccan basalts, Vindhyan carbonates, sediments, and alluvial deposits (Sharma and Subramanian, 2008; Dessert et al., 2001) affecting the pH. Modifications also occur along the river system’s long course e.g., by a number of hydrothermal springs which have been reported along the Narmada-Tapti lineament (Minissale et al., 2000), besides the human-caused factors (Qasim et al., 2022). This estuary to be grouped along with the other anthropogenically affected much smaller NW estuaries may indicate the extent of anthropogenic flows into the estuary (Qasim et al., 2022).

According to Eq. 5, the stoichiometry of the overall reaction indicates that the liberation of HCO₃⁻ and H₄SiO₄ is in the 1:2 ratio, and since DIC is dominated by HCO₃⁻, Si and DIC should be expected to covary. However, there was no relationship between the two except in SW (Fig. S3). This may be attributed to the mineral diversity of the basin rocks/soils subjected to weathering in the other regions.

4.2. CDOM's potential in estuarine mixing studies:

The CDOM was linearly related to salinity (Fig. 3a) in the NE and SW estuaries. Conservative behavior of CDOM has been reported extensively in literature within estuaries over broad salinity ranges when the mixing of river and sea waters is conservative (e.g., Guo et al., 2007). Conservative behavior within each group of estuaries during the monsoon season may indicate that the watershed characteristics are nearly uniform within these groups. The non-conservative behavior of CDOM in the SE and NW estuaries may be related to the uniqueness of each estuary in terms of discharge, weathering inputs and anthropogenic inputs. CDOM has been reported in a few of the NE (Godavari, Rushikulya estuaries) and SW (Mandovi/Zuari) estuaries of the Indian peninsula (Pandi et al., 2021b; Sanyal et al. 2020; Dias et al., 2020, 2017; Menon et al., 2011). In the Godavari estuary, according to our knowledge, a maximum CDOM of 5.76 m^{-1} has been recorded in any of the Indian estuaries (Pandi et al., 2021b). The estuary showed both conservative and non-conservative behavior depending on whether a broad salinity range was covered (during the post-monsoon season) or a small salinity range was covered (during peak monsoon season) (Pandi et al., 2021b). The CDOM was low in the Krishna estuary of NE (average, 1.7848 m^{-1}) and in the Cauvery estuary (1.1546) of SE and this was attributed to the release of dam-stored water upstream during our sampling period, due to the late arrival of monsoon. During 2014 when the sampling was done, the summer monsoon arrived particularly late and although Krishna (NE) and Cauvery (SE) rivers rise in the Western Ghats where the monsoon strikes first on the Indian mainland (Mangalaa et al., 2017), both estuaries showed (low) concentrations due to prolonged storage in the reservoirs. In the Godavari estuary, the lowest CDOM (during a full year) was observed at the time of the dam-stored water's discharge into the estuary during the dry season when the river discharge nearly ceased (Pandi et al., 2021b).

4.2.1. $S_{300-500}$ and SR of CDOM as indicators of anthropogenic organic inputs:

The Spectral slope ($S_{300-500}$) of $0.0163 \pm 0.0011 \text{ nm}^{-1}$ and 0.0157 ± 0.0010 in the NE and SW estuaries respectively agrees closely with the $S_{300-500}$ of world average river water (0.0016 , Bowers and Brett, 2008). The $S_{300-500}$ was higher in the SE and NW estuaries (0.0172 ± 0.0005 and $0.0149 \pm 0.0014 \text{ nm}^{-1}$ respectively) which indicated that the CDOM may be of different composition i.e., of lower molecular weight DOM than that of NE and SW estuaries (Pandi et al., 2021a; Coble, 2007). CDOM was also high in SE estuaries ($4.7827 \pm 2.9731 \text{ m}^{-1}$, Fig. 3a), and taken together with elevated concentrations of NH_4^+ , TA, DIC in them (Table S2) inferred significant organic anthropogenic inputs in them.

In the NW estuaries, CDOM was lowest ($1.4195 \pm 0.6480 \text{ m}^{-1}$) but the *SR* was high in both SE (1.1 ± 0.11) and NW (1.23 ± 0.42) estuaries with reference to the linear regression of *SR* on salinity in the NE+SW estuaries (eq. 1, Fig. 4a). The *SR* is believed to indicate MW and to trace photochemical and microbial history of DOM (Fichot and Benner, 2012, 2011). Due to the bacterial and photochemical processing of the anthropogenically derived DOM, *SR* increases to > 1 (Gold et al., 2020; Yi et al., 2011). The higher *SR* of SE and NW estuaries indicated their DOM to be of lower MW than in NE and SW estuaries. The CDOM of NE (*SR*, 0.91 ± 0.05) and SW (0.87 ± 0.08) estuaries (Fig. 2c) was fresh from terrestrial (mainly plant) sources i.e., of higher MW. This DOM is aromatic (derived from lignin) and made up of larger polymers of HA/FA brought in by the river water (Fichot and Benner, 2012), and resistant to photochemical or microbial processes (Coch et al., 2019). The moderately lower *SR* (and $S_{300-500}$) of the SW estuaries than that of the NE estuaries (Fig. 2d, Table S2) may reflect the SW estuaries' fresher FA/HA richer DOM extracted from the thicker vegetation and soils along the slopes of the Western Ghats than the coastal plains-dominated Eastern Ghats (Mangalaa et al., 2017).

The depleted $\delta^{13}\text{C}$ of POC (4 of the 14 samples had $\delta^{13}\text{C}$ in the range -30.1‰ to -26.3‰ in SE and 3 of the 6 samples had $\delta^{13}\text{C}$ in the range -29.9‰ to -26.3‰ , Fig. S1f). Comparatively, the typical estuarine value is -24‰ (Middelburg and Nieuweuwenhuize, 1998; Thornton and McManus, 1994). The low $\delta^{13}\text{C}$ values were associated with enriched $\delta^{15}\text{N}$ of PON (9.7 to 23.1‰ , 6 of 14 samples, Fig. S1g) which are higher than typical estuarine values ($3\text{-}5\text{‰}$, Thornton and McManus, 1994) in the SE estuaries. Such large $\delta^{15}\text{N}$ of PON values are mainly contributed by pollution by local industrial and domestic sewage effluents. In addition to this, high NH_4^+ (Fig. S1a), DIC (Fig. 2a) and TA (Fig. S1h) concentrations were also observed in the SE and NW estuaries which further indicated that possible input of anthropogenic pollution into the SE and NW estuaries.

4.3. CDOM as a proxy of organic alkalinity in the NE & SW estuaries:

The contributions of CDOM to DIC, calculated from eq. 2, are of similar magnitude as the difference between the TA determined experimentally and TA obtained by summation of inorganic weak acid anions, at coastal stations close to estuaries (Yang et al., 2015). The present findings on CDOM contributions to DIC and TA agree with the literature reports. For example, an 'Organic alkalinity' (DOM alkalinity, org-alk or A_{org} , the acronym used in this paper) has been reported to comprise ca 78% of the total alkalinity at low salinity to less than 0.4% at the coastal ocean endmember, in the St. John Estuary (Hunt et al., 2022). The high contributions in the SE estuaries may be attributed to fulvic acids, as in the case of A_{org} in the Baltic Sea (Hammer et al, 2017; Ulfsbo et al., 2015; Kuliński et al., 2014), and pharmaceuticals (Herber, 2009) originated from the huge aquaculture

industry and the small size of the (SE) estuaries. The CDOM (A_{org}) of NE and SW estuaries is likely the higher MW (and aromatic) congener of fulvic acids, namely the humic acids.

The model (eq. 2) appears to be supported by the fact that the CDOM contribution to DIC relates to DIC in the NE+SW samples which were involved in the model (Fig. 5c). The tight relationship in the case of the unmodeled SE+NW samples may indicate that the DIC contribution by CDOM is controlled by the CDOM (DOM) itself which is of high SR (>1.1) in these (polluted) estuaries. A similar argument for pH's contribution to DIC (Fig. 5d) may indicate that the pH may be controlling its own contribution to DIC in the unpolluted, low pH (average =7.00) SW estuaries. The eq. 2 calculates that the pH would rise by 0.67 in the NE estuaries if the average DIC remained as it were i.e., 1484 μM from the current pH of 7.65 and by 0.38 in the SW estuaries (612 μM , 7.00 respectively) in the absence of CDOM contribution. And that with CDOM increasing from its present average levels of 2.8375 m^{-1} (NE estuaries) and 1.6485 m^{-1} (SW) by 10%, the DIC would increase by 56.7 μM and 32.9 μM i.e., by 4% and 5.6% in the respective estuaries considering that the pH remained unchanged. Similarly, a decrease of pH by 1% from its present average levels would cause a decrease in the DIC by 71.5 μM and 65.5 μM i.e., by 5% and 11% in the NE and SW estuaries respectively, considering that the CDOM remained unchanged.

Thus, the effect of perturbations is felt more in the SW estuaries than in NE estuaries. Sarma et al. (2012) showed that Indian estuaries are characterized by high supersaturation of CO_2 and perennial efflux to the atmosphere. Since the developed model is for the open system, the decrease in pH shifts the dissolved inorganic carbon system towards the formation of CO_2 , which increases the gradient of pCO_2 levels between water and atmosphere, leading to the efflux of CO_2 to the atmosphere and decrease in DIC. The results agree with the trends predicted by numerical simulations of the seawater buffer capacity with changing A_{org} (Hu, 2020). The eq. 2 is empirical and not analytical as the contributions calculated for pH and CDOM do include contributions from other species based on their concentrations, acid-base equilibria, ionic interactions and solubility characteristics.

Considering a likely pK_a of 6.5 for the CDOM, the pK_a is close to that of H_2CO_3 (6.35, ACS, 2022), and there may be a few other species that could potentially influence its calculated (as per eq. 2) contribution to DIC. The role of CDOM is indirectly justified by the fact that soil organic carbon (SOC) is known to be adsorbed, stabilized and rendered unreactive to the environmental chemical reagents (Torn et al., 1997) and that when this layer is removed (by the erosional and abrasive forces of rain and stream in the river basin), the inner silicate minerals get exposed. CDOM has been observed to co-vary with H_4SiO_4 in the Godavari estuary, and the authors justified it through a laboratory experiment mimicking estuarine aquatic conditions. They concluded that CDOM 'co-leached' with

H₄SiO₄ from the estuarine silt (Pandi et al., 2021b). There are several oceanographically significant, more common (soluble) inorganic weak acid - weak base species e.g., HCO₃⁻ (pK_a, 25°C, 10.33), H₄SiO₄ (9.8), NH₄⁺ (9.24), H₃BO₃ (9.15), H₂CO₃ (7.35), H₂PO₄⁻ (7.21) and H₂S (7.05) (ACS, 2022) which may potentially influence the contribution of pH in the model (eq. 2) according to their abundance and environmental variability.

The significance of A_{org}, especially that coming from organic acids e.g., HA in the estuarine buffer mechanism remains largely unknown currently (Hu, 2020). In such a scenario, the empirical model for DIC in terms of CDOM (DOC) (eq. 2) is expected to be a step forward. The role played by CDOM may explain the lag between DIC, pH and alkalinity in the low salinity regions such as estuaries and coasts (salinity < ~20x10⁻³, Cai et al., 2021) which are the hotspots of A_{org} (Hunt et al., 2022; Kerr et al., 2021; Hu, 2020). Further, as the influence of regional factors on the broad structure of CDOM is limited (Coble, 2007), the role of CDOM (DOM) in the estuarine DIC dynamics could be extended in other watersheds as well.

4.4. Can CDOM be useful to predict Ocean Acidification (OA)?

In order to address this question, (TA-DIC) was considered as an intermediary. The first attempt was to show that (TA-DIC) is a proxy of acidification, and then to show that CDOM (*SR*) is related to (TA-DIC).

4.4.1. (TA-DIC) as a proxy of Ocean Acidification:

The (TA-DIC) versus pH₂₅ plot (Fig. 6a) is like a seawater titration curve as increasing (TA-DIC) is equivalent to incremental additions of base (CO₃²⁻, Xue and Cai, 2020; Broecker and Peng, 1982) to (the acidic) river water. This plot is considered useful in deciphering acidification mechanisms and predicting the future development of ocean acidification (OA) (Xue and Cai, 2020). The upper regression relationship in Fig. 6a is in agreement with the oceanic relationship derived by Xue and Cai (2020) and the datapoints covered by it (N=33) are of pH range from 6.54 to 8.66 over a broad salinity range (0.43 to 31.68 x10⁻³) and were from the NE and SE estuaries mostly. This group of samples are Class 1 in Fig. 6a. Regarding the lower regression line in Fig. 6a (Class 3, its data (eq. 4, N=12) is on the acidic side (pH₂₅, 6.2 to 7.0 mostly), and from the upstream stations of the west coast estuaries mostly. The two regression lines are nearly parallel (slopes, 0.001528 and 0.001584 pH(TA-DIC)⁻¹ respectively). It meant that the rate of increase of pH with (TA-DIC) or vice versa (6.55 and 6.31 μM(0.01pH)⁻¹ respectively) was nearly the same in the two groups.

In Fig. 6a, the upper regression line extending to the left and the lower regression line extending to the right of the titration-like curve is to be explained in terms of estuary-specific inputs and processes. For

example, in the Penna and Haldia upstream waters, (TA-DIC) was marginally lower despite high alkalinity (averages, 3508 and 2287 μM respectively) as the DIC values were also high (3523 and 2196 μM respectively). The Ganges water reaching the Hooghly estuary (of which Haldia is a part) carries with it the weathered products from limestone (Samanta and Dalai, 2016). In the case of Penna estuary, intense aquaculture activity in which lime and limestone are used as liming materials in the maintenance and renewal of aquaculture ponds (Boyd and McNevin, 2015), and the pharmaceuticals (Herber, 2009) may be contributing to excess (TA-DIC). In the upper estuary stations of NW (Fig. 6a), DIC was lower which could be due to increased biological production (DIC uptake). High chl-a at these stations (average, 18.3 mgm^{-3}) compared to the others (3.2) (Fig. S1e) supported the inference. Fig. 6a further suggests that in Classes 1 and 3, buffering of pH is happening, and that HA may likely supplement the carbonate system here (Xu et al., 2021; Hu, 2020; Theng, 2012).

As the environmental conditions existing in the estuaries are a little varied (Xue et al., 2018), the DIC and TA-induced buffer or sensitivity factors are generally similar in magnitude (Eggleston et al., 2010), and the pH perturbation is likely due to DOM changes. The CDOM owing to in situ processes taking place on phytoplankton is labile and reported to have two distinct pK_a values of 4.4–4.9 and 6.1–6.9 corresponding to the C-term and N-term respectively of proteins (Ko et al., 2016) unlike the (somewhat higher) pK_a of ex situ CDOM (see above). The Class 4 samples in Fig. 6a were disconnected from Classes 1 to 3. These samples had excess DIC over alkalinity implying an overwhelming of the natural sources (e.g., carbonate system, borate etc.) by anthropogenic sources. The biogeochemical processes affecting the (TA-DIC) vs pH_{25} relationship and the changes in acidification and the consequent concentration of TA, DIC etc. harmful to the environment (Cai et al., 2021) are likely confined to estuaries of the NW region.

In summary, the DIC equilibria in the solution phase are likely influenced by (i) H_4SiO_4 - related CDOM in samples falling along the two regression lines (Fig. 6a) and a role for the river-originated humic acids in buffering (Classes 1 and 3), (ii) mixing with seawater in the case of constant TA-DIC group of samples whose in situ CDOM had little buffering ability (Class 2), and (iii) excess acidification by anthropogenic inputs beyond the ability of estuarine water to cope up with (Class 4). At most estuaries, Classes 1 to 3 samples prevailed which indicates that acidification is likely contained within the estuary itself by the carbonate buffer system. The Class 4 samples in which excessive DIC led to strongly negative TA-DIC values, were present downstream of Narmada (salinity, 28.1×10^{-3}) and Tapti (20.11) estuaries. The coastal region may receive inputs of this acidified water.

4.4.2. *SR* of CDOM supports coastal acidification:

In the (TA-DIC) Classes 1 and 3 (NE and SW estuaries) of Fig. 6a, the distribution of *SR* versus (TA-DIC) (Fig. 6b) gave a further insight into the structural changes of CDOM. *SR* increased significantly with (TA-DIC) ($p < 0.001$) i.e., as salinity and pH increased and with them, the carbonate system was enriched. The *SR* has earlier been proposed as an indicator of increasing proportion of lower MW CDOM/DOM (Helms et al., 2008). Higher (TA-DIC) in both Classes 1 and 3 and of Class 1 over Class 3 samples is thus likely caused by the degradation of CDOM. The Class 3 samples which were from the upstream samples of SW estuaries were inferred above to be constituted of freshly extracted DOM from the soils and plant matter of the Western Ghats. This DOM is fresher and of higher MW than that of Class 1 samples (NE samples, higher water temperature). The rise of pH_{25} in Classes 1 and 3 versus (TA-DIC) being gentle infers that the associated decrease of CDOM MW is slow and the structural change (degradation) is slow and that the buffering property of the CDOM is retained in these two Classes. In the case of Class 2 samples (SW downstream) which are of nearly constant (TA-DIC) and *SR*, the CDOM which is labile (being of phytoplankton origin) sourced from the sea. In these samples, over small changes of *SR* (MW) and (TA-DIC), pH changed much and argues for the loss of buffering capacity of this labile CDOM (DOM) due to its tendency for more extensive degradation than the CDOM (DOM) of Classes 1 and 3. Labile CDOM can readily produce DIC (Amaral et al., 2021). Uniquely for the Class 4 samples, the *SR* was anomalous, being either too high or low with reference to the salinity-*SR* regression line (eq. 1, Fig. 4a) in high saline downstream samples close to the salinity of coastal seawater. The criterion of anomalous *SR*, unaccounted by salinity, could probably infer possibility of acidification of the coastal sea.

A summary of the results on the role of CDOM on DIC in the Indian estuaries described in Section 4.3 is presented in Fig. 7a and the findings on estuarine acidification in terms of the Classes 1 to 4 (this Section) in Fig. 7b.

5. Conclusions:

The Study on eighteen Indian estuaries has revealed two dominant types: those influenced by continental weathering inputs (northeast NE and southwest SW estuaries) and those dominated by anthropogenic inputs (southeast SE and northwest NW estuaries). Key findings are briefly as follows:

- CDOM (Chromophoric Dissolved Organic Matter) characteristics differ between the two types of estuaries. In the river-fresh NE and SW estuaries, the CDOM is mainly made up of humic components. These humic components have a higher molecular weight (MW) compared to the estuaries in the

southeast (SE) and northwest (NW), which are affected by human activities and have CDOM primarily composed of non-humic components.

- An empirical model has been proposed that relates Dissolved Inorganic Carbon (DIC) to CDOM and pH in unpolluted estuaries. CDOM plays a pivotal role in predicting DIC levels in these estuaries.
- The calculated CDOM contribution to DIC may largely represent 'organic alkalinity' (A_{org}), indicating the importance of CDOM in influencing the dissolved CO_2 system.
- The relationship between the difference between Total Alkalinity and DIC (TA-DIC) and pH_{25} (pH at $25^\circ C$) extends its applicability to estuaries with lower salinities. The previous assumption that it applies only to marine regions with higher salinities is exceptionable.
- Estuarine waters in NE and SW estuaries are well-buffered due to their longer weathering histories, and changes in DOM MW are moderate, thanks to the stability of the humic and fulvic acids present.
- In contrast, abrupt changes in DOM occur when originating from the productive (Arabian) Sea, characterized by its labile nature when phytoplankton originated. This labile DOM has limited buffering capacity.
- The Spectral Slope ratio (SR) emerges as a crucial parameter in understanding these processes and holds potential to detect aquatic acidification by referring to the SR -salinity baseline distribution.

The study demonstrates CDOM's utility in tracking human-caused pollution in Indian estuaries and establishes the link between estuarine CDOM, the CO_2 system, 'organic alkalinity' and water acidification.

Acknowledgements: Authors thank Professor Damien Cardinal (DC) for accommodating one of us (GC) for samples collection, their on-site processing and for comments on an initial draft of the MS. Laboratory facilities and the invitation to DC as a Visiting Professor by Andhra University are gratefully acknowledged. Financial assistance No. F&A:XII:D2:023 from the INCOIS-MoES, and the award of Honorary Professorship by Andhra University (to NSS) are also gratefully acknowledged. This is a joint contribution of Andhra University, National Centre for Polar and Oceanographic Research (No. . . .), Centre for Marine Living Resources & Ecology (No. . . .), and National Institute of Oceanography (No. . . .).

Declaration of generative AI and AI-assisted technologies in the writing process : During the preparation of this work, the author(s) used ChatGPT Tool in order to improve the readability of the Conclusions section. After using this tool, the author(s) reviewed and edited the content as needed and take(s) full responsibility for the content of the publication.

References:

- American Chemical Society, pka-compilation-williams.pdf (organicchemistrydata.org), accessed April 4, 2023.
- Amaral V, Ortega T, Romera-Castillo C, Forja J, 2021. Linkages between greenhouse gases (CO₂, CH₄, and N₂O) and dissolved organic matter composition in a shallow estuary, *Sci Total Environ*, 788: 147863.
- Asmala E, Stedmon CA, Thomas DN, 2012. Linking CDOM spectral absorption to dissolved organic carbon concentrations and loadings in boreal estuaries, *Estuar Coast Shelf Sci*, 111: 107-117,
- Bhattacharya R, Osburn CL, 2021. Chromophoric dissolved organic matter composition and load from a coastal river system under variable flow regimes, *Sci Total Environ*, 760: 143414.
- Bowers DG, Brett HL, 2008. The relationship between CDOM and salinity in estuaries: An analytical and graphical solution, *J Mar Sys*, 73 (1-2): 1-7.
- Boyd CE, McNevin AA, 2015. Chemicals in Aquaculture, In: *Aquaculture, Resource Use, and the Environment* (CE Boyd, AA McNevin, eds). <https://doi.org/10.1002/9781118857915.ch9>
- Bricaud A, Morel A, Prieur L, 1981. Absorption by dissolved organic matter of the sea (yellow substance) in the UV and visible domain. *Limnol Oceanogr* 26(1): 43–53
- Broecker WS, Peng TH, 1982. Tracers in the sea. The Lamont-Doherty 502 Geological Observatory, Palisades, New York, 1-690 pp
- Bunn SE, Loneragan NR, Kempster MA, 1995. Effects of acid washing samples on stable isotope ratios of C and N in penaeid shrimps and seagrass: Implications for food web studies using stable isotopes, *Limnol Oceanogr*, 40: 622–625.
- Cai W-J, Feely RA, Testa JM, Li M, Evans W, Alin SR, Xu Y-Y, Pelletier G, Ahmed A, Greeley DJ, Newton JA, Bednaršek N, 2021. Natural and Anthropogenic Drivers of Acidification in Large Estuaries, *Ann Rev Mar Sci*, 13(1): 23-55
- Chandra S., Ghosh K, Varadachari C, 2014. Weathering of Silicate Minerals by Humic Acids: II. Nature of Cation Solubilisation from Hornblende and Biotite and Characteristics of the Residual Products. *Clay Res*, 33: 46-63.
- Chari NVHK, Sarma NS, Pandi SR, Murthy KN, 2012. Seasonal and spatial constraints of fluorophores in the midwestern Bay of Bengal by PARAFAC analysis of excitation emission matrix spectra. *Estuar Coast Shelf Sci* 100:162–171.
- Chari NVHK, Keerthi S, Sarma NS, Pandi SR, Chiranjeevulu G, Kiran R, Umadevi K, 2013. Fluorescence and absorption characteristics of dissolved organic matter excreted by phytoplankton species of western Bay of Bengal under axenic laboratory condition. *J Exp Mar Biol Ecol*, 445:148–155.
- Charlson RJ, Rodhe H, 1982. Factors controlling the acidity of natural rainwater. *Nature* 295: 683–685.

- Chiranjeevulu G, Murty KN, Sarma NS, Kiran R, Chari NVHK, Pandi SR, Venkatesh P, Annapurna C, Rao KN, 2014. Colored dissolved organic matter signature and phytoplankton response in a coastal ecosystem during mesoscale cyclonic (cold core) eddy. *Mar Environ Res* 98:49–59.
- Choppin GR, Kullberg L, 1978. Protonation thermodynamics of humic acid, *J Inorg Nucl Chem*, 40(4): 651-654.
- Coble P, Zepp R, Zika, R, 2004. CDOM in the ocean: Transformation processes and their effects on optical properties. *Mar Chem*, 89: 1-1. 10.1016/j.marchem.2004.06.001.
- Coble PG, 2007. Marine Optical Biogeochemistry: The Chemistry of Ocean Color. *Chemical Reviews*, 107: 402-418.
- Coch C, Juhls B, Lamoureux SF, Lafrenière MJ, Fritz M, Heim B, Lantuit H, 2019. Comparisons of dissolved organic matter and its optical characteristics in small low and high Arctic catchments, *Biogeosciences*, 16: 4535–4553.
- Coplen TB, 1996. New guidelines for reporting stable hydrogen, carbon and oxygen isotope-ratio data, *Geochim Cosmochim Acta*, 60: 3359–3360.
- Davies G, Ghabbour EA (Editors), 1998. “Humic substances : structures, properties and uses.”. Royal Society of Chemistry: Cambridge, UK. 241 pp.
- Dessert C, Dupre B, Francois LM, Schott J, Gaillardet J, Chakrapani G, Bajpai S, 2001. Erosion of Deccan Traps determined by river geochemistry: impact on the global climate and the $^{87}\text{Sr}/^{86}\text{Sr}$ ratio of seawater. *Earth Planet Sci Letts*, 188: 459–474.
- Dias AB, Thayapurath S, Sahay A, Chauhan P, 2017. Contrasting characteristics of colored dissolved organic matter of the coastal and estuarine waters of Goa during summer. *Indian J Geo Mar Sci*, 46: 860–870.
- Dias A, Kurian S, Thyapurath S, 2020. Influence of environmental parameters on bio-optical characteristics of colored dissolved organic matter in a complex tropical coastal and estuarine region. *Estuar Coast Shelf Sci*, 242:106864. Doi: 10.1016/j.ecss.2020.106864
- Dickson AG, 1981. An exact definition of total alkalinity and a procedure for the estimation of alkalinity and total inorganic carbon from titration data. *Deep Sea Res Part A*, 28: 609–623.
- DOE (Department of Energy), 1998. Determination of total alkalinity in sea water. In: *Hand Book of Methods for the Analysis of the Various Parameters of the Carbon Dioxide System in Seawater. Version 2* (eds. Dickson AG, C Goyet). Carbon Dioxide Information and Analysis Center, Oak Ridge, TN, ORNL/CDIAC-74, pp. 56-85.
- Egleston ES, Sabine CL, Morel FMM, 2010. Revelle revisited: buffer factors that quantify the response of ocean chemistry to changes in DIC and alkalinity, *Global Biogeochem Cycles*, 24: GB1002
- Fichot CG, Benner R, 2011. A novel method to estimate DOC concentrations from CDOM absorption coefficients in coastal waters, *Geophys Res Letts* 38(3): L03610.
- Fichot CG, Benner R, 2012. The spectral slope coefficient of chromophoric dissolved organic matter ($S_{275-295}$) as a tracer of terrigenous dissolved organic carbon in river-influenced ocean margins, *Limnol Oceanogr*, 57: 1453–1466.

- Goering J, Alexander V, Haubenstock N, 1990. Seasonal variability of stable carbon and nitrogen isotope ratios of organisms in a North Pacific Bay, *Estuar Coast Shelf Sci*, 30: 239–260.
- Gold AC, Thompson SP, Magel CL, Piehler MF, 2020. Urbanization alters coastal plain stream carbon export and dissolved oxygen dynamics. *Sci Total Environ* 747:141132. <https://doi.org/10.1016/j.scitotenv.2020.141132>
- Grunert B, Tzortziou M, Neale P, Menendez A, Hernes P, 2021. DOM degradation by light and microbes along the Yukon River - coastal ocean continuum. *Sci Rep*, 11: 10236.
- Guo W, Stedmon C, Han Y, Wu F, Yu X, Hu M, 2007. The conservative and non-conservative behavior of chromophoric dissolved organic matter in Chinese estuarine waters, *Mar Chem*, 107: 357-366.
- Hammer K, Schneider B, Kuliński K, Schulz B, Detlef E, 2017. Acid-base properties of Baltic Sea dissolved organic matter, *J Mar Sys*, DOI:10.1016/j.jmarsys.2017.04.007
- Hartmann J, Jansen N, Dürr HH, Kempe S, Köhler P, 2009. Global CO₂-consumption by chemical weathering: What is the contribution of highly active weathering regions? *Global Planet Change*, 69(4), 185–194.
- Hartmann, J, Lauerwald R, Moosdorf N, 2014. A Brief Overview of the Global River Chemistry Database, GLORICH. *Procedia Earth Planet Sci*, 10: 23–27.
- Helms JR, Stubbins A, Ritchie JD et al., 2008. Absorption spectral slopes and slope ratios as indicators of molecular weight, source, and photobleaching of chromophoric dissolved organic matter, *Limnol Oceanogr*, 53: 955–969.
- Herber T, 2009. Organic compounds used in aquaculture. In: *Hormones and Pharmaceuticals Generated by Concentrated Animal Feeding Operations, Emerging Topics in Ecotoxicology 1* (ed. Shore, L. S. and Pruden, A.), pp. 95–120. Springer Science and Business Media, New York, USA
- Hosen JD, McDonough OT, Febria CM, Palmer MA, 2014. Dissolved organic matter quality and bioavailability changes across an urbanization gradient in headwater streams. *Environ Sci Technol.*, 48(14): 7817-7824.
- Hu X, 2020. Effect of Organic Alkalinity on Seawater Buffer Capacity: A Numerical Exploration. *Aquatic Geochemistry* <https://doi.org/10.1007/s10498-020-09375-x> 1 3
- Hunt CW, Salisbury JE, Vandemark D, 2022. Controls on buffering and coastal acidification in a temperate estuary. *Limnol Oceanogr*, 67: 1328-1342.
- IWAI, Inland Waterways Authority of India, 2016. Consolidated Environmental Impact Assessment Report of National Waterways-1, Volume-6, Ministry of Shipping, Government of India, May 2016, <https://iwai.nic.in/about-us>
- Kerr DE, Brown PJ, Grey A, Kelleher BP, 2021. The influence of organic alkalinity on the carbonate system in coastal waters, *Mar Chem*, 237: 104050.
- Khullar DR, 2014. *India: A Comprehensive Geography*, Kalyani (pub), India, 868 pp.
- Ko YH, Lee K, Eom KH, Han I, 2016. Organic alkalinity produced by phytoplankton and its effect on the computation of ocean carbon parameters. *Limnol Oceanogr*, 61: 1462–1471.

- Kuliński K, Schneider B, Hammer K, Machulik U, Schulz-Bull D, 2014. The influence of dissolved organic matter on the acid–base system of the Baltic Sea. *J Mar Sys*, 132: 106–115.
- Mangalaa KR, Cardinal DM, Brajard J, Rao DB, Sarma NS, et al., 2017. Silicon cycle in Indian estuaries and its control by biogeochemical and anthropogenic processes. *Cont Shelf Res*, 148: 64–88.
- Mariotti A, 1983. Atmospheric nitrogen is a reliable standard for natural ^{15}N abundance measurements, *Nature*, 303, 685–687.
- Menon HB, Sangekar NP, Lotliker AA, Vethamony P, 2011. Dynamics of chromophoric dissolved organic matter in Mandovi and Zuari estuaries – A study through in situ and satellite data, *ISPRS J. Photogramm. Rem Sens*, 66(4), 545–552.
- Middelburg JJ, Nieuweuwenhuize J, 1998. Carbon and nitrogen stable isotopes in suspended matter and sediments from the Schelde Estuary, *Mar Chem*, 60, 217–225.
- Middelburg JJ, Soetaert K, Hagens M, 2020. Ocean alkalinity, buffering and biogeochemical processes. *Rev Geophys*, 58: e2019RG000681.
- Minissale A, Vaselli O, Chandrasekharam D, Magro D, Tassi F, Casiglia A., 2000. Origin and evolution of ‘intracratonic’ thermal fluids from central-western region peninsular India. *Earth Planet Sci Lett*, 181: 377–394.
- Mostofa KU, Liu C-Q, Mottaleb MA, Wan G, Ogawa H, Vione D, Yoshioka T, Wu F, 2013. Dissolved Organic Matter in Natural Waters. 10.1007/978-3-642-32223-5_1.
- Nisha BK, Balakrishna K, Udayashankar HN, Manjunatha BR, 2021. Chemical weathering and carbon dioxide consumption in a small tropical river catchment, southwestern India, *Aquat Geochem*, DOI:10.1007/s10498-021-09394-2
- Pandi SR, Kiran R, Sarma NS et al., 2014. Contrasting phytoplankton community structure and associated light absorption characteristics of the western Bay of Bengal, *Ocean Dyn*, 64: 89–101.
- Pandi SR, Chari NVHK, Sarma NS, Tripathy SC, Chiranjeevulu G, Das S, 2021a. A review of Estuarine CDOM dynamics of East Coast of India influenced by hydrographical forcing, Ch 14, In: *Estuar Biogeochem Dyn East Coast India*, S Das (ed), Springer (pub), 223–237.
- Pandi SR, Chari NVHK, Sarma NS, Chiranjeevulu G, Kiran R, Murthy KN, Venkatesh P, Lotliker AA, Tripathy SC, 2021b. Characteristics of conservative and non-conservative CDOM of a tropical monsoonal estuary in relation to changing biogeochemistry, *Reg Stud Mar Sci*, 44: 101721.
- Paul S, Sharma T, Saikia D, Saikia P, Borah D, Baruah MK, 2015. Evaluation of pKa Values of Soil Humic Acids and their Complexation Properties. *International J Plant Soil Sci*, 6: 218–228.
- Perminova IV, Frimmel FH, Kudryavtsev AV, Kulikova NA, Abbt-Braun G, Hesse S, Petrosyant VS, 2003. Molecular weight characteristics of humic substances from different environments as determined by size exclusion chromatography and their statistical evaluation. *Environ Sci Technol*, 37(11): 2477–2485.
- Pinnegar JK, Polunin NVC, 1999. Differential fractionation of $\delta^{13}\text{C}$ and $\delta^{15}\text{N}$ among fish tissues: Implications for the study of trophic interactions, *Funct Ecol*, 13: 225–231.

- Qasim A, Singh SP, Ahmad N *et al.* 2022. Inter-estuarine and seasonal to decadal variations of heavy metal pollution in the Gulf of Cambay, India. *Environ Monitor Assess*, 194: 36.
- Rao GD, Sarma VVSS, 2015. Contribution of N₂O emissions to the atmosphere from Indian monsoonal estuaries, *Tellus-B*, 65: 19660.
- Rao GD, Sarma, VVSS, 2016. Variability in concentrations and fluxes of methane in the Indian estuaries, *Estuaries and Coasts*, 39, 1639-1650.
- Samanta S, Dalai TK, 2016. Dissolved and particulate Barium in the Ganga (Hooghly) River estuary, India: Solute-particle interactions and the enhanced dissolved flux to the oceans, *Geochim Cosmochim Acta*, 195: 1–28.
- Sanyal P, Ray R, Paul M, Gupta VK, Acharya A, Bakshi S, Jana TK, Mukhopadhyay SK, 2020. Assessing the Dynamics of Dissolved Organic Matter (DOM) in the Coastal Environments Dominated by Mangroves, Indian Sundarbans. *Front Earth Sci* 8: 1–21.
- Sarma VVSS, Viswanadham R, Rao GD, Prasad VR, Kumar BSK, Naidu SA, Kumar NA, Rao DB, Sridevi T, Krishna MS, Reddy NPC, Sadhuram Y, Murty TVR, 2012. Carbon dioxide emissions from Indian monsoonal estuaries, *Geophys. Res. Lett.*, 39, L03602, doi:10.1029/2011GL050709.
- Sarma VVSS, Krishna MS, Prasad VR, Kumar BSK, Naidu SA, Rao GD, Viswanadham R, Sridevi T, Kumar PP, Reddy NPC, 2014. Distribution and sources of particulate organic matter in the Indian monsoonal estuaries during monsoon. *J. Geophys. Res. (G: Biogeosciences)*, 119(11): 2095-2111.
- Sarma NS, Pandi SR, Chari NVHK *et al.*, 2018. Spectral modelling of estuarine coloured dissolved organic matter. *Curr Sci* 114:1762–1767.
- Schnoor JL, Stumm W, 1986. The role of chemical weathering in the neutralization of acidic deposition, *Swiss J Hydrol*, 48: 171-195.
- Seidel M, Yager P L, Ward ND, Carpenter EJ, Gomes HR, Krusche AV *et al.*, 2015. Molecular-level changes of dissolved organic matter along the Amazon river-to-ocean continuum. *Mar Chem*, 177: 218–231.
- Shank G, Zepp R, Whitehead R, Moran MA, 2005. Variations in the spectral properties of freshwater and estuarine CDOM caused by partitioning onto river and estuarine sediments. *Estuarine, Coastal and Shelf Science*, 65: 289-301.
- Sharma SK, Subramanian V, 2008. Hydrochemistry of the Narmada and Tapti Rivers, India. *Hydrological Processes*, 22(17): 3444–3455.
- Shetye S, Naik H, Kurian S, Shenoy DM, Kuniyil N, Fernandes M, Hussain A, 2020. pH variability off Goa (eastern Arabian Sea) and the response of sea urchin to ocean acidification scenarios. *Mar Ecol*, 41: n pag.
- Soli AL, Byrne RH, 2002. CO₂ system hydration and dehydration kinetics and the equilibrium CO₂/H₂CO₃ ratio in aqueous NaCl solution, *Mar Chem*, 78 (2-3): 65-73.
- Soman MK, Kumar KK. 1990. Some aspects of daily rainfall distribution over India during the southwest monsoon season, *Int J Clim*, 19, 299–311.

Song S, Wang ZA, Eagle MG, Kroeger KD, Chu SN, Li D, Liang H, 2000. An important biogeochemical link between organic and inorganic carbon cycling: Effects of organic alkalinity on carbonate chemistry in coastal waters influenced by intertidal salt marshes, *Geochim Cosmochim Acta*, 275: 123-139.

Subramanian V 1993. "Sediment load of Indian Rivers." *Curr Sci* 64 (11/12): 928–30.

Theng BKG, 2012. Humic substances, Ch 12. In: *Developments in Clay Science*, BKG Theng (Editor), Elsevier, 4:391- 456.

Thornton SF, McManus J, 1994. Application of organic carbon and nitrogen stable isotope and C/N ratios as source indicators of organic matter provenance in estuarine systems: Evidence from the Tay Estuary. *Scotland, Estuarine Coastal Shelf Sci.*, 38, 219–233.

Torn M, Trumbore S, Chadwick O, Vitousek PM, Hendricks DM, 1997. Mineral control of soil organic carbon storage and turnover. *Nature*, 389: 170–173.

Ulfso A., Kuliński K, Anderson LG, Turner DR, 2015. Modelling organic alkalinity in the baltic sea using a humic-pitzer approach. *Mar Chem*, 168: 18–26.

Vaidyanathan A, 2013. *Water Resources of India*, Oxford Univ Press (India), ISBN: 9780198090427, 272 pp.

Vidal L, Lambert T, Cotovicz Jr L, Bernardes M, Sobrinho R, Thompson F, Garcia G, Knoppers B, Gatts P, Ramos RC, Abril G, Rezende C, 2023. Seasonal and diel modulation of DOM in a mangrove-dominated estuary, *Sci Total Environ*, 857: 159045.

Visser SA., 1964. A physicochemical study of the properties of humic acids and their changes during humification. *J Soil Sci*, 15: 202-219.

Xu J, Mohamed E, Li Q, Lu T, Yu H and Jiang W, 2021. Effect of Humic Acid Addition on Buffering Capacity and Nutrient Storage Capacity of Soilless Substrates, *Front. Plant Sci*, 12: 644229.

Xue L, Cai W-J, 2020. Total alkalinity minus dissolved inorganic carbon as a proxy for deciphering ocean acidification mechanisms, *Mar Chem*, 222: 103791.

Xue L, Cai WJ, Takahashi T, Gao L, Wanninkhof R, Wei M, Li K, Feng L, Yu W, 2018. Climatic modulation of surface acidification rates through summertime wind forcing in the Southern Ocean. *Nat Comm*, 9(1): 3240.

Yang B, Byrne RH, Lindemuth M, 2015. Contributions of organic alkalinity to total alkalinity in coastal waters: A spectrophotometric approach, *Mar Chem*, 176: 199-207.

Yi Y, Zhang S, Zhuo J, Huang L, Guo W, 2011. Absorption Properties of Chromophoric Dissolved Organic Matter in Highly-Polluted Yundang Lagoon, China, *Procedia Env Sci*, 10 (C): 2554-2559.

Legend to Figures

Fig. 1: The 18 river estuaries of the Indian peninsula: NE=northeast, SE=southeast, SW=southwest, NW=northwest sectors (estuary names: HD-Haldia, SR-Subarnarekha, MNMahanadi, RK-Rushikulya, GV-Godavari, KN-Krishna, PN-Penna, PY-Ponnaiyar, VL-Vellar, CR-Cauvery; KC-Kochi, NV-Netravati, KL-Kali, ZR-Zuari, MV-Mandovi, TT-Tapti, NDNarmada and MS-Mahisagar)

Fig. 2: Distribution of (a) DIC (μM), (b) salinity ($\times 10^{-3}$) versus pH plot in the NE and SW estuaries, and distributions of (c) CDOM (a_{350} , m^{-1}), and (d) Spectral slope ratio (SR). The (a), (c) and (d) are detailed distributions in the NE, SE, SW and NW estuaries. (The sample numbers on X-axis: SNos 1, 5, 9, . . . 69 are upstream, 2, 6, 10, . . . 70 the midstream riverward, 3, 7, 11, . . . 71 the midstream sea-ward and 4, 8, 12, . . . 72 the downstream/seaward stations).

Fig. 3: Variability of CDOM (m^{-1}) against salinity ($\times 10^{-3}$) in (a) NE and SW, (b) SE and NW estuaries, and against (c) H_4SiO_4 (μM) and (d) DIC (μM) in all 4 sectoral (NE, SE, SW, NE) estuaries

Fig. 4: Variability of Spectral slope ratio (SR) against (a) salinity ($\times 10^{-3}$), H_4SiO_4 (μM) and (c) DIC (μM) in all 4 in the estuaries, and (d) Verification of the estimated DIC using eq. 2 (see Text) against DIC (observed) (The outlier is a regression outlier with the residual more or less than the predicted value by at least 50%)

Fig. 5: CDOM's contribution to DIC: (a) μM , (b) Percent of DIC, the remaining being accounted by pH, (c) Dependence of DIC (μM) contributed by CDOM on CDOM (m^{-1}), and (d) Dependence of DIC (μM) contributed by pH on pH

Fig. 6: TA-DIC (μM) plots: (a) against pH₂₅, showing classification of different estuarine samples into Class 1 - mostly NE and SE estuaries), Class 2 - mostly midstream of SW, Class 3 - mostly upstream of SW and NW and Class 4 - Outliers of NW in which acidification unbuffered acidification is taking place, and (b) against SR of Classes 1 to 3 samples.

Fig. 7: Summary of CDOM (m^{-1})-DIC (μM) coupling: (a) The contribution of organic alkalinity (A_{org}) to DIC in the NE, SE, SW and NW estuaries calculated from the model (eq. 2, see Text). (the blue color indicates natural as major and pink, the anthropogenic as significant inputs), (b) The distribution of Classes 1 to 4 of Fig. 7a in the 18 Indian estuaries. The geographic coordinates of the mid-stream and downstream stations are moved slightly with reference to the upstream station coordinates by $X(Y) \pm n \times 0.2$ where X and Y are longitude and latitude respectively of the upstream station and $n=1$ (river-ward midstream station), 2 (seaward midstream station) and 3 (downstream i.e., seaward station), for better visibility of the variations.

Fig. S1: Distribution of TA, H_4SiO_4 (μM), POC and PON data of the NE, SE, SW and NW estuaries separately. Outlier data are not shown to improve visibility of the non-outlier data.

Figure 1:

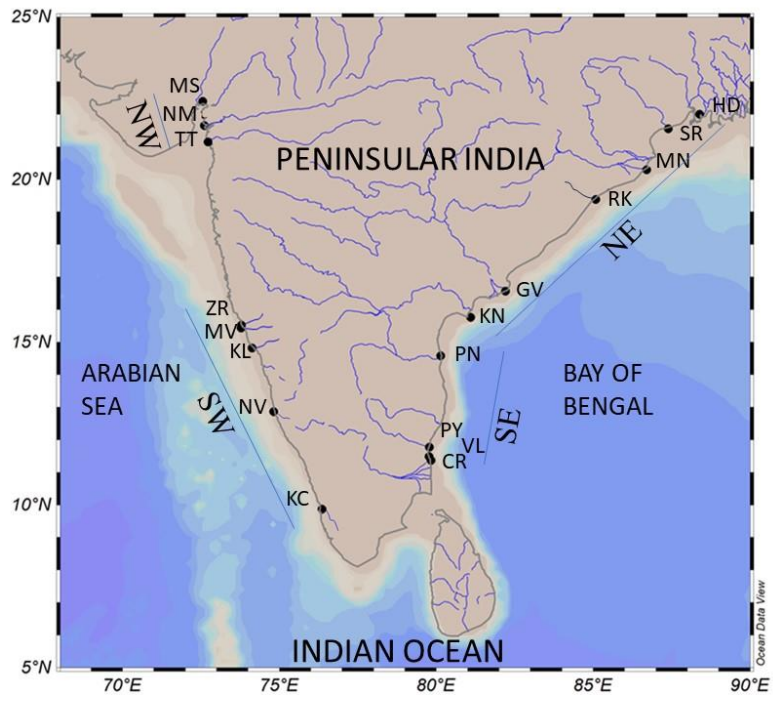


Figure 2:

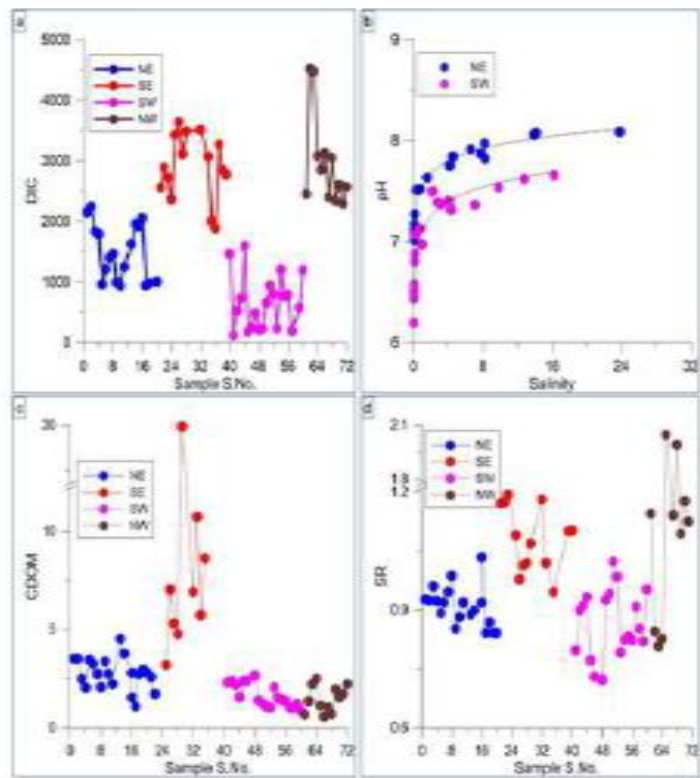


Figure 3:

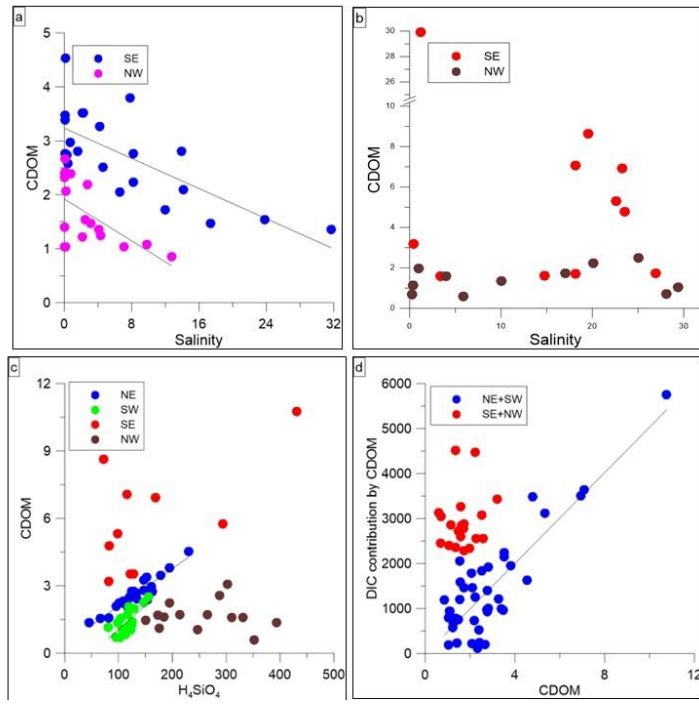


Figure 4:

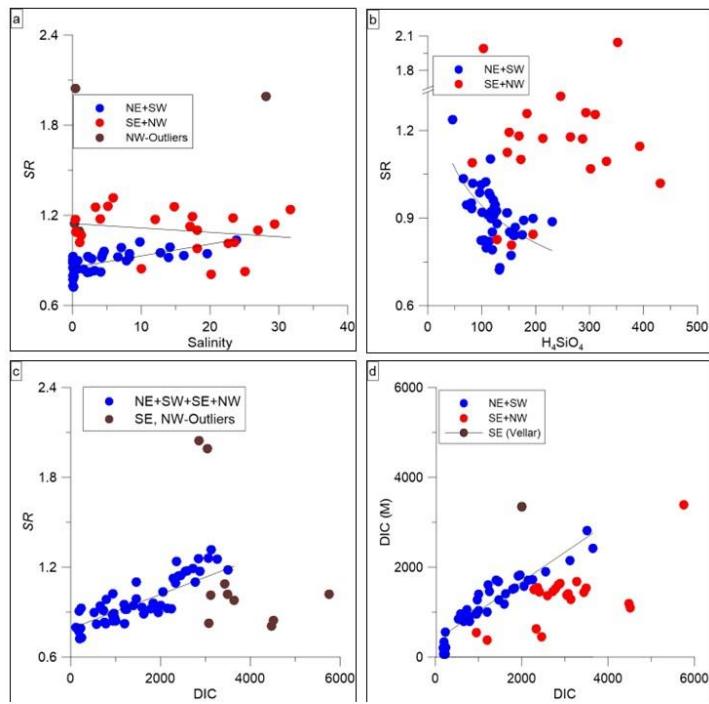


Figure 5:

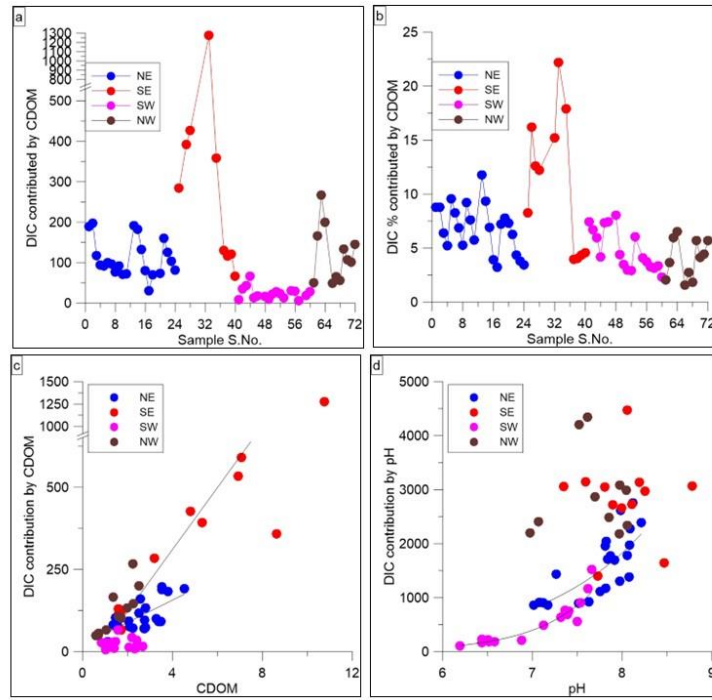


Figure 6:

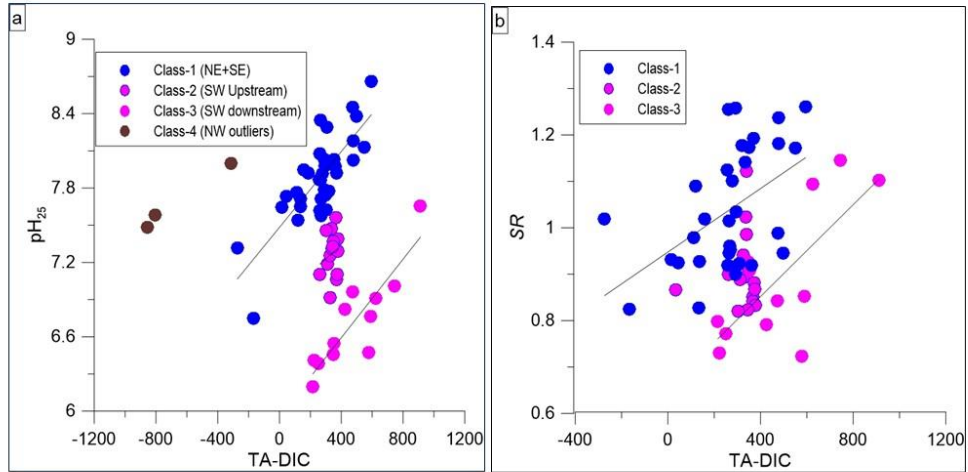
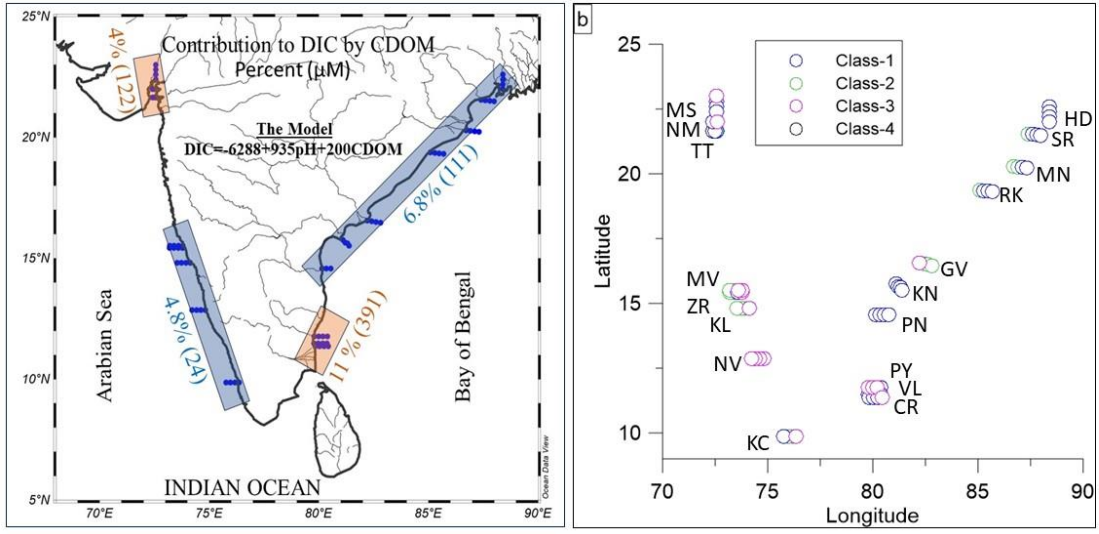
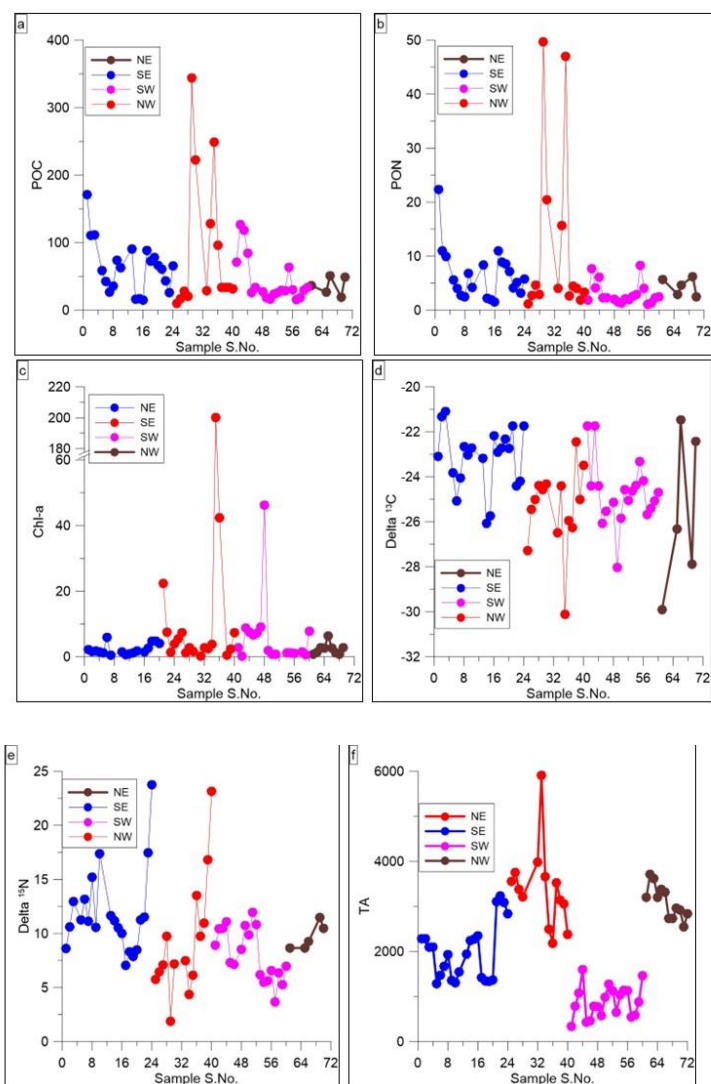


Figure 7:



Supplementary Fig. S1: Distribution of a) POC, b) PON, c) Chl-a and d) $\delta^{13}\text{CPOC}$, e) $\delta^{15}\text{N}$ and f) TA in the Indian estuaries.



Supplementary Fig. S2: The relationship between salinity and pH

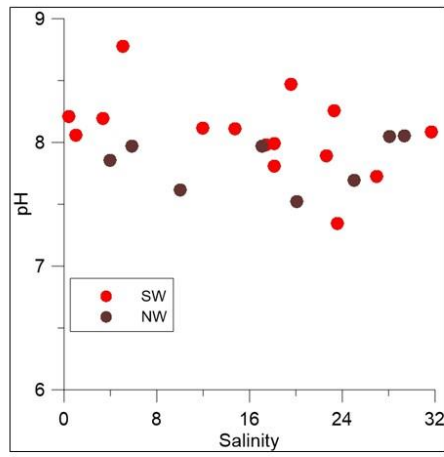


Fig. S2

Supplementary Fig. S3: Relationship between DIC and silicate in the Indian estuaries

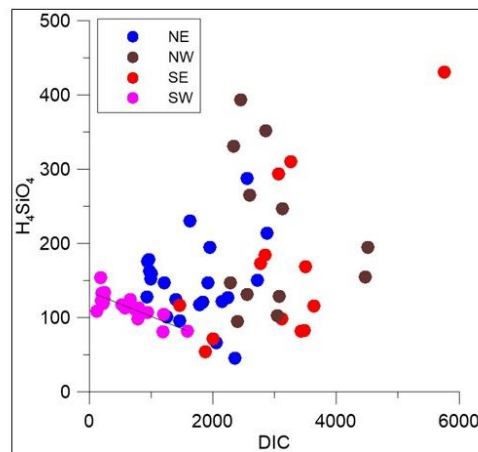


Fig. S3

Supplementary Figure S4: Relationship between pH and SR in the Indian estuaries

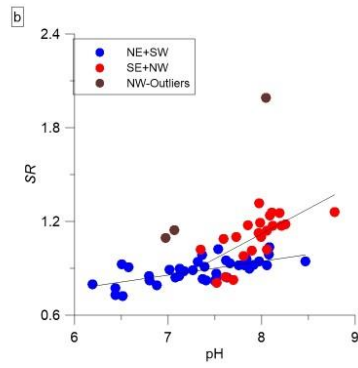


Fig. S4

Supplementary Figure S5: Relationship between pH and DIC contribution by CDOM

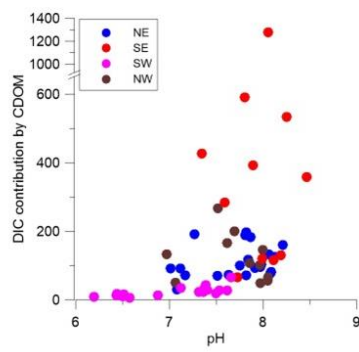


Fig. S5

Table S1: Hydrogeological characteristics of Rivers

Estuary	Origin	Length (Km)	Catchment area (*10 ³ Km ²)	Discharge (km ³ yr ⁻¹)	Industries in the catchment areas
Haldia	Tangrakhal, WB (joins Hooghly, a distributary of Ganga)	24	NA	50.45	Oil refinery, Petrochemical, Chemical, Sugar
Subarnarekha	Piska, Ranchi., JH	395	18.95	12.36	Mining (Copper, Uranium ores)
Mahanadi	Chiroli Hills, Western Ghats, CG	858	141.59	66.82	Iron, Steel
Rushikulya	Rishi Hill, Eastern Ghats, OD	165	8.96	NA	Chemical, Sugar, Mining
Godavari	Brahmagiri Mountain, Western Ghats, MH	1,465	312.81	110.53	Agricultural, Agro-based, Paper
Krishna	Mahabaleswar, Western Ghats, MH	1,400	258.95	51.78	Textiles, Sugar, Chemicals, Cement
Penna	Nandi Hills, Western/Eastern, KA	597	55.21	6.32	Aquaculture, Sea food, Granite, Steel
Ponnaiyar	<u>Nandidurg</u> , Western/Eastern Ghats, KA	400	3.69	0.64	Sewage (of <u>Bangalore city</u>), Sugar
Vellar	<u>Shevaroy Hills</u> , TN	210	8.92	NA	Ceramics, aquaculture
Cauvery	Talakaveri, Western Ghats, KA	765	81.16	21.35	Paper, Sugar, Chemical, Cotton, Steel, Cement
Kochi Backwaters	Western Ghats, KL	900	NA	12.33	Plastic, Rubber, Chemical, Petrochemical
Netravati	Bangrabalige valley, Western Ghats, <u>KA</u>	103	3.66	NA	Agro-based
Kali	Diggi, <u>Western Ghats</u> , KA	184	48.51	4.79	Sand mining, Chemicals, Petroleum
Zuari	Hemad-Barshem, <u>Western Ghats</u> , Goa	34	NA	3.25	Pharmaceuticals
Mandovi	<u>Bhimgad</u> , <u>Western Ghats</u> , KA	77	NA	3.31	Pharmaceuticals
Narmada	Maikal hill, Shahdol Dt., MP	1,312	95.88	38.35	Petrochemicals
Tapti	Multai, Betul Dt., MP	724	65.15	15.42	Textile, Pharmaceuticals, Plastics, Paper, Sugar, Cereals, Oil, Wood
Mahisagar	Sardarpur, Dhar Dt., MP	580	39.71	12.08	Agro-based, Textile, Leather, Plastic, Rubber, Drugs, Pharmaceuticals

NA= Data not available; WB: West Bengal, JH: Jharkhand, CG: Chhattisgarh, OD: Odisha, MH: Maharashtra, KA: Karnataka, KL: Kerala and MP: Madhya Pradesh.

Table S2: Complete Data Table

Estuary	Sample No.	Salinity x 10 ⁻³	Temp °C	pH	Tchl a mg m ⁻³	NH ₄ ⁺ μM	SiO ₄ μM	POC mg l ⁻¹	PON mg l ⁻¹	¹³ C ‰	¹⁵ N ‰	TA μM	DIC μM	a ₃₅₀ m ⁻¹	SR
Haldia	1	2.17	31.5	7.809	2.28	0.84	121.96	171.48	22.35	-23.10	8.62	2283	2146	3.5236	0.93
	2	2.27	30.8	7.822	1.60	0.88	127.51	110.46	11.01	-21.32	10.63	2290	2245	3.5236	0.92
	3	4.59	33.5	7.84	1.82	0.92	121.23	111.26	9.96	-21.09	12.94	2102	1833	2.5103	0.96
	4	6.61		7.914	1.53	1.42	117.61					2098	1789	2.0497	0.92
Subarnarekha	1	0.09	31.5	7.014	1.15	0.42	177.99	58.69	5.63	-23.83	11.27	1286	959	3.4775	0.89
	2	4.22	34	7.754	6.00	1.04	146.83	42.50	4.00	-25.07	13.15	1474	1213	3.2703	0.92
	3	8.23		7.971	0.45	0.96	124.86	26.86	2.74	-24.06	11.13	1666	1403	2.7636	0.95
	4	14.15		8.075		1.19	95.88	35.54	2.46	-22.65	15.20	1937	1462	2.0957	0.99
Mahanadi	1	0.09	28.6	7.118		1.31	152.15	74.13	6.80	-23.03	10.57	1363	995	3.3854	0.85
	2	0.09	29.5	7.171	1.46	1.57	128.00	62.50	4.24	-22.73	17.37	1310	936	2.7636	0.88
	3	8.23	30.1	7.819	0.61	0.96	100.71					1550	1249	2.2339	0.92
	4				0.94										
Rushikulya	1	0.14	30.2	7.267	1.17	0.73	230.63	90.75	8.42	-23.18	11.63	1937	1627	4.5369	0.89
	2	7.83	30.4	7.87	1.77	1.42	195.13	16.05	2.17	-26.08	11.18	2247	1956	3.8000	0.90
	3	13.95	30.5	8.058		1.34	147.32	16.75	1.94	-25.74	10.51	2278	1917	2.8097	0.92
	4	23.83	32	8.084	1.48	0.31	65.93	15.08	1.52	-22.17	10.00	2349	2056	1.5430	1.03
Godavari	1	0.11	32.7	7.079	2.61	0.42	175.33	88.38	11.01	-22.90	7.03	1417	944	1.1054	1.84
	2	0.34	33	7.512	4.82	0.42	162.53	72.63	8.88	-22.73	8.30	1348	972	2.7406	0.87
	3	0.71	29.6	7.52	4.83	0.46	161.08	78.24	8.52	-22.33	7.86	1334		2.9709	0.84
	4	1.59	29.6	7.631	4.13	0.54	158.91	66.36	7.18	-22.74	8.46	1366	1000	2.8097	0.84
Krishna	1	0.43	30.4	8.212	22.42	0.38	287.39	60.82	4.08	-21.74	11.26	3104	2555	2.5794	1.17
	2	11.98	30.7	8.117	7.50	0.81	213.49	43.28	5.18	-24.40	11.53	3234	2883	1.7273	1.17
	3	17.40	29.1	7.983	1.30	0.61	150.45	25.92	3.16	-24.21	17.45	3089.841	2719.361	1.4739	1.19
	4	31.68	29.2	8.087	3.92	0.19	45.89	65.31	5.78	-21.74	23.78	2840.778	2362.596	1.3588	1.24
Penna	1	0.46	28.3	7.592	5.55	9.02	82.11	10.16	1.14	-27.29	5.73	3553.805	3434.527	3.2012	1.09
	2	18.14	27.8	7.807	7.40	13.36	115.44	17.13	2.73	-25.45	6.44	3755.762	3644.625	7.0702	0.98

	3	22.61	27.2	7.895	1.25	9.60	98.77	28.03	4.63	-25.02	7.10	3380.521	3114.988	5.3199	1.02
	4	23.56	27	7.347	2.72	9.02	83.08	20.13	2.92	-24.39	9.74	3215.28	3488.876	4.7902	1.02
Ponnaiyar	1	1.21	31.6		1.59	7.83	302.12	344.05	49.68	-24.58	1.88			29.9390	1.07
	2									-24.32	7.16				
	3				0.28										
	4	23.29	30	8.255	2.73	11.52	169.05	222.87	20.42			3985.8	3507.042	6.9320	1.18
Vellar	1	1.04	32.3	8.057	2.55	1.00	431.08	29.11	4.03	-26.48	7.50	5911.496	5752.9	10.7550	1.02
	2	5.09	32.8	8.78	3.80	1.11	293.42	128.02	15.70	-24.41	4.38	3659.415	3064.809		1.26
	3	19.57	30.8	8.469	200.00	4.92	71.97	248.69	46.99	-30.12	6.13	2499.846	2003.003	8.6363	0.95
	4	32.23	32.8	7.741	42.40	0.88	53.85	96.30	2.66	-25.95	13.51	2184.656	1883.436		
Cauvery	1	3.35	32.6	8.193		0.84	310.57	33.39	4.49	-26.27	9.76	3528.113	3266.419	1.5891	1.26
	2	14.76	30.3	8.11	0.56	1.04	184.26	33.44	4.03	-22.45	10.94	3138.02	2847.266	1.6121	1.26
	3	18.14	30	7.994	2.35	0.96	172.67	33.34	1.85	-25.02	16.81	3055.263	2777.432	1.7042	1.10
	4	26.94	29.6	7.726	7.31	0.42	116.40	31.59	3.38	-23.49	23.14	2377.615	1464.878	1.7273	1.10
Kochi	1	0.03	24.6	6.194	2.79	0.84	108.43	71.15	1.90	-21.74	8.90	334.1557	118.6733	2.3260	0.80
	2	0.75	26.5	7.125	0.23	4.99	117.37	126.58	7.64	-24.40	10.44	789.4439	528.7439	2.3951	0.90
	3	2.79	26.4	7.389	8.85	6.18	111.09	118.59	4.14	-21.74	10.47	1078.28	729.61	2.1879	0.91
	4	16.18	26.1	7.66	7.53	4.99	81.63	84.38	6.09	-24.40	11.07	1602.75	1589.359	1.5660	0.93
Netravathi	1	0.05	28.2	6.436	6.61	1.27	154.32	26.03	2.31	-26.06	7.31	432.3136	181.0624	2.3951	0.77
	2	0.07	26.8	6.438	7.17	0.50	133.79	33.80	2.33	-25.53	7.13	467.677	244.196	2.4182	0.73
	3			6.613	9.04							781.989	478.8624		
	4	0.10	27.6	6.513	46.26	0.88	132.83	27.30	2.00	-25.13	8.54	780.6817	202.8018	2.6715	0.72
Kali	1	0.04	28.2	6.504	1.97	0.73	125.10	18.60	1.52	-28.03	10.76	580.6544	233.4752	1.4048	0.93
	2	4.34	29.1	7.316	0.77	1.38	124.37	16.26	1.34	-25.84	9.89	985.0973	658.5847	1.2436	0.94
	3	9.80	29	7.533	0.80	1.80	107.47	23.81	2.12	-24.58	11.96	1275.264	938.2189	1.0824	1.02
	4	7.08	28.2	7.361		1.31	113.26	25.92	1.97	-25.04	10.81	1135.053	795.4238	1.0364	0.99
Zuari	1	0.19	28.6	6.878		1.92	119.30	29.71	2.60	-24.64	6.17	651.5013	227.2214	2.0727	0.79
	2	2.47	28.3	6.799	1.14	1.88	104.33	28.90	2.89	-24.38	5.49	1034.009	1200.134	1.5430	0.82
	3	3.16	29.9	7.367	1.21			63.78	8.31	-23.33	5.61	1135.42	758.0499	1.4739	0.83

	4	4.08	29.9	7.403	1.02	1.96	98.77	29.88	4.06	-24.19	6.56	1127.316	781.8739	1.3588	0.82	
Mandovi	1	0.07	27	6.575		0.58	122.44	15.73	1.09	-25.68	3.67	541.683	188.3585	1.0364	0.89	
	2	0.17	27	6.797	1.56	1.11	119.54	18.37	1.34	-25.42	6.34	590.0512		1.0364	0.91	
	3	2.13	27.7	7.498	0.68	1.11	113.26	29.81	2.30	-25.08	5.26	882.0599	579.8166	1.2206	0.85	
	4	12.73	27.5	7.617	7.78	0.92	80.66	33.52	2.51	-24.70	6.96	1463.531	1193.731	0.8521	0.82	
Tapti	1	0.27	29	7.068	0.82	1.34	393.16	36.50	5.68	-29.90	8.66	3201.91	2455.659	0.6909	1.99	
	2	10.02	27.2	7.615	1.37	10.68	195.13					3709.153	4513.904	1.3588	1.15	
	3	20.11	27.3	7.521	2.72	4.49	155.28					3621.903	4475.785	2.2339	0.85	
	4	25.05	27.9	7.696	2.59	2.00	128.72					3207.636	3073.296	2.5103	0.81	
Narmada	1	0.38	28.6		6.39	1.04	351.87	26.63	2.89	-26.32	8.66	3379.942	2854.264	1.1515	0.95	
	2	5.86	28.3	7.972	2.60	4.19	246.57	51.14	4.64	-21.46	9.27	3320.607	3133.154	0.5988	2.05	
	3	29.38	28.3	8.056	1.22	1.00	94.91					2736.653	2402.353	1.0594	1.32	
	4	28.10	28.2	8.048	0.72	2.00	103.12					2729.951	3042.92	0.7139	1.14	
Mahisagar	1	0.97	29.2	6.973	2.72	1.27	331.34	19.32	6.24	-27.89	11.48	2962.307	2337.283	1.9806	0.83	
	2	3.99	30.4	7.855		2.57	264.68	48.61	2.49	-22.43	10.46	2918.605	2598.603	1.5891	1.09	
	3	17.06	31.7	7.969		1.88	147.32					2542.809	2286.062	1.7273	1.18	
	4			7.997		0.61	131.13					2839.613	2561.378	2.2569	1.13	
Notes: Blank cells, No Data; In column B, 1=upstream, 2 & 3=mid-stream; 4=downstream of all estuaries;																

Table S3: Concentrations (Averages) in different salinity bands of NE and SW estuaries

	Salinity band (x 10 ⁻³)	No. of observations	Salinity (x 10 ⁻³)	Temperature (°C)	pH	Alkalinity (µM)	DIC (µM)
NE	<2	9	0.40	30.57	7.39	1607.76	1248.95
	2-5	3	3.31	32.45	7.81	2037.63	1860.02
	5-10	4	7.72	30.25	7.89	1890.70	1599.86
	10-15	3	13.36	30.60	8.08	2483.46	2087.98
	15-20	1	17.40	29.10	7.98	3089.84	2719.36
	20-25	1	23.83	32.00	8.08	2349.67	2056.01
	25-30	-	-	-	-	-	
	30-35	1	31.68	29.20	8.09	2840.78	2362.60
SW	<2	11	0.78	27.27	6.74	657.41	331.27
	2-5	4	3.24	28.98	7.28	1032.78	795.69
	5-10	2	8.44	28.60	7.45	1205.16	866.82
	10-15	1	12.73	27.50	7.62	1463.53	1193.73
	15-20	1	16.18	26.10	7.66	1602.75	1589.36
	20-25	-	-	-	-	-	-
	25-30	-	-	-	-	-	-
	30-35	-	-	-	-	-	-
NE-SW	<2	NE/SW: 9/11	-0.38	3.29	0.65	950.35	917.68
	2-5	3/4	0.08	3.47	0.53	1004.85	1064.33
	5-10	4/2	-0.72	1.65	0.45	685.54	733.03
	10-15	3/1	0.63	3.10	0.47	1019.93	894.24
	15-20	1/1	1.22	3.00	0.32	1487.09	1130.00
NE-SW Average	0-20	20/19	0.16	2.90	0.48	1029.55	947.86

-No data; Nos in bold are mentioned in Text.